

Cite this: *J. Mater. Chem. A*, 2022, 10, 11823

## Hydrogels for underwater adhesion: adhesion mechanism, design strategies and applications

Xintao Ma,<sup>†a</sup> Xun Zhou,<sup>†a</sup> Junjie Ding,<sup>a</sup> Bin Huang,<sup>a</sup> Puying Wang,<sup>a</sup> Yi Zhao,<sup>a</sup> Qiyu Mu,<sup>a</sup> Shaohua Zhang,<sup>\*a</sup> Chunguang Ren<sup>\*b</sup> and Wenlong Xu<sup>id</sup><sup>\*a</sup>

A hydrogel is a polymer material with a porous network structure, which allows the hydrogel to swell rapidly underwater without dissolving. This unique property of hydrogels lays the foundation for their application in underwater adhesion. However, due to the existence of the hydration layer, the interaction between the hydrogel and the adherend surface is seriously hindered, and the underwater adhesion ability of the hydrogel is severely weakened. In the past few decades, various hydrogels for underwater adhesion have been developed, among which the underwater adhesion mechanisms of natural organisms have provided a steady stream of inspiration for researchers to design underwater adhesion hydrogels. In this review, we first summarize the adhesion mechanism and design strategies of underwater adhesion hydrogels, and then introduce the currently common experimental methods to test the adhesion strength and adhesion toughness of underwater adhesion hydrogels. According to the development trend in recent years, we summarize the common application fields of underwater adhesion hydrogels. Finally, we present our views on the challenges of hydrogels for underwater adhesion, and provide an outlook on future research directions. This review provides a comprehensive overview of underwater adhesion hydrogels, which will provide rational guidelines for the design and fabrication of underwater adhesion hydrogels.

Received 12th March 2022  
Accepted 9th May 2022

DOI: 10.1039/d2ta01960d

rsc.li/materials-a

### 1. Introduction

Currently, most of the commercially available adhesives can exhibit high adhesion strength in a dry environment. However, when working underwater, the adhesive needs to be immersed

in an aqueous medium to achieve bonding, but achieving adhesion in water is more challenging than in air. When most materials are exposed to water, a hydrated layer forms on the surface, which severely hinders the bonding between the adhesive and the substrate.<sup>1–3</sup> In addition, existing polymer adhesives are subject to water attack in water and can swell to failure. Therefore, the development of underwater adhesives is urgent.

As a soft material with a three-dimensional network structure, hydrogels have been widely used in the fields of

<sup>a</sup>School of Chemistry and Materials Science, Ludong University, Yantai, 264025, China. E-mail: zhangshaohua@ldu.edu.cn; xuwenlong@ldu.edu.cn

<sup>b</sup>Yantai Institute of Materia Medica, Yantai, 264000, China. E-mail: cgren@yimm.ac.cn

<sup>†</sup> These authors contributed equally.



*Xintao Ma is an undergraduate student of Grade 2, and he is currently pursuing his bachelor degree in Polymer Materials and Engineering at Ludong University. His research interests focus on the fabrication of polymer hydrogels and their applications.*



*Xun Zhou is an undergraduate student of Grade 2, and she is currently pursuing her bachelor degree in Polymer Material and Engineering at Ludong University. Her research interests focus on the fabrication of polymer hydrogels and their applications.*

bioadhesion,<sup>4,5</sup> 3D printing,<sup>6</sup> environmental protection<sup>7,8</sup> and intelligent regulation.<sup>9–11</sup> Hydrogels can swell rapidly in water without dissolving, thus laying the foundation for the application of hydrogels in underwater adhesion. Although remarkable progress has been made in hydrogels for underwater adhesion, it is still extremely challenging to construct a hydrogel with stable and durable underwater adhesion. Many marine organisms (such as mussels, sandcastle worms and barnacles) can tightly adhere to various underwater substrates by secreting liquid protein glues containing various amino acid residues.<sup>12–19</sup> For example, sandcastle worms utilize six secreted adhesion proteins to achieve underwater adhesion. Inspired by the underwater adhesion strategies of these marine organisms, significant progress has been made in the design of various underwater adhesion hydrogels.<sup>20–25</sup> However, when the hydrogel adheres to the adherend underwater, the contact area between the hydrogel and the adherend is reduced due to the existence of the hydration layer, which seriously hinders the underwater adhesion effect of the hydrogel, so design and fabrication of underwater adhesion hydrogels face enormous challenges.<sup>26–29</sup>

All the hydrogel systems summarized in this review adhered to the adherend in the underwater environment. In some cases, the hydrogels for underwater application were solidified in air prior to contact with water; these hydrogels also adhere well when applied underwater, and they were different from those

summarized in this review. This review doesn't address the biological applications (such as wound healing, bone adhesion and hemostatic adhesion) of hydrogels, because the adhesion of hydrogels to tissues is wet adhesion, and this review focuses on the summary of underwater adhesion. In this review, we discuss the adhesion mechanisms, design strategies and characterization of hydrogels for underwater adhesion, and then extend our discussion to the application of underwater adhesion hydrogels. In Section 2, according to the steps of hydrogel underwater adhesion, we first summarize the ways of removing the hydration layer, including repelling and absorbing the hydration layer. The interaction between hydrogels and adherends underwater is demonstrated, which is mainly dependent on covalent bonds and intermolecular forces, such as hydrogen bonds, electrostatic interactions, hydrophobic interactions,  $\pi$ - $\pi$  stacking, cation- $\pi$  interactions and metal coordination. The synergistic effect of these intermolecular forces provides the hydrogel with stable and long-term underwater adhesion. According to the underwater adhesion mechanism of hydrogels, different design strategies are discussed for the gel-type and sol-type hydrogels in Section 3. Section 4 is devoted to summarizing common underwater adhesion characterization methods that may be used to test the adhesion strength and adhesion toughness of hydrogels. In Section 5, we summarize practical applications of underwater adhesion hydrogels including underwater adhesives, underwater motion detection, marine



*Junjie Ding is an undergraduate student of Grade 1, and she is currently pursuing her bachelor degree in Polymer Material and Engineering at Ludong University. Her research interests focus on the fabrication of polymer hydrogels and their applications.*



*Dr Chunguang Ren is currently a Senior Engineer in Yantai Institute of Materia Medica. He obtained his PhD in materials science from Nara Institute of Science and Technology. Since joining Yantai Institute of Materia Medica in 2015, he has worked in a variety of research areas including the topic of functional hydrogels and the design of biomaterials from self-assembling peptides.*



*Dr Shaohua Zhang received her PhD in Colloid and Interface Chemistry from Shandong University in 2012. And now, she is a lecturer at Ludong University. Her recent research interests focus on the fabrication of polymer hydrogels and peptide hydrogels and their applications.*



*Dr Wenlong Xu received his PhD in Physical Chemistry from Shandong University in 2016. He worked in Shandong Luye Pharmaceutical Co., Ltd for two years, focusing on drug development of a long-acting and targeting drug delivery system. In 2018, he joined Ludong University and focused on the fabrication of polymer hydrogels and peptide hydrogels and their applications.*

resource exploration and underwater coatings. Finally, we present our views on the challenges of hydrogels for underwater adhesion, and provide an outlook on future research on underwater adhesion of hydrogels. We hope that the insights we have provided can offer inspiration and valuable references for the design and fabrication of underwater adhesion hydrogels.

## 2. Underwater adhesion mechanism for underwater adhesion hydrogels

The key to the underwater adhesion of hydrogels lies in the removal of the hydration layer and the formation of covalent bonds/intermolecular forces. In this section, we divide the current methods of removing the hydration layer into the repelling of the hydration layer and the absorption of the hydration layer, which is also the first step of underwater adhesion. The formation of covalent bonds/intermolecular forces is then detailed in the second step.

### 2.1. Hydration layer

In the field of underwater adhesion of hydrogels, the hydration layer is considered as a water film between the hydrogel and the adherend, which seriously hinders the adhesion of the hydrogel to the adherend.<sup>29–33</sup> Therefore, removing the hydration layer is the first step in underwater adhesion. In this section, two hydration layer removal methods are introduced and a concise overview of the research progress of interfacial water removal is given.

**2.1.1. Repelling the hydration layer.** Repelling the hydration layer can be achieved through different scales.<sup>29</sup> At the molecular level, the hydrophobic groups can remove the hydration layer from the interface by hydrophobic interactions and keep the water away from the contact interface after the hydrogel adheres underwater. Therefore, hydrophobic solvent and hydrophobic monomers were usually used for repelling the hydration layer by hydrogels.<sup>1,29,34,35</sup> Spraying a hydrophobic solvent on the surface of the hydrogel can form a thin liquid layer, with which the contact angle between the hydrophobic thin layer and water is small. When external pressure is applied to the hydrogel, the hydration layer can be destroyed and discharged from the surface of the adherend (Fig. 1A).<sup>34</sup> In addition, the hydrophobic thin layer can increase the molecular mobility of uncross-linked molecules, making it easy to form covalent bonds or intermolecular forces with functional groups on the surface of the adherend.<sup>34</sup> For hydrophobic monomers, monomers with long carbon chains or aromatic ring structures are often used to provide hydrophobic interactions.<sup>26,36,37</sup> When the hydrogel is in contact with water, the monomers with long carbon chains can rapidly aggregate and form a coacervate, thereby repelling the water molecules on the surface of the adherend, making the hydrogel and the adherend stick together through other intermolecular forces without being destroyed by water.<sup>36</sup> The aromatic ring possesses hydrophobicity and the structure of the aromatic ring endows it with a variety of functional groups, so the monomer with the aromatic ring can repel

the hydration layer and form covalent bonds/intermolecular forces by itself.<sup>26</sup>

The biomimetic microstructure works well in repelling the hydration layer.<sup>38,39</sup> The design of the biomimetic microstructure is inspired by the adhesive disc of the clingfish and the surface structure of tree-frog footpads, both of which possess hexagonal microstructures that can quickly repel the hydration layer. Therefore, the hydrogel and the adherend are in direct contact, which increases the actual contact area between the hydrogel and the adherend (Fig. 1B).<sup>38</sup>

**2.1.2. Absorbing the hydration layer.** Compared with the method of repelling the hydration layer, the method of absorbing the hydration layer is simple and has lower requirements on the design of the hydrogel.<sup>40</sup> The absorption of the hydration layer is based on the fact that the hydrogel contains highly hygroscopic materials, and the moisture on the interface is absorbed when the hydrogel is in contact with the hydration layer. Wang *et al.* dissolved poly(vinylpyrrolidone) (PVP, as a hygroscopic polymer) in acrylic acid together with a cross-linker and photoinitiator, followed by *in situ* photocuring (IPC) to fabricate a hygroscopic adhesive. Fluorescence performance showed that water with fluorescent dye initially stayed at the interface of the substrate and was finally absorbed into the hydrogel, which demonstrated that the hydrogel possessed the ability to absorb the interface moisture (Fig. 1C).<sup>41</sup> Cong *et al.* designed an underwater adhesion hydrogel that was functionalized by anthracene-based polyethyleneimine with water-absorbing polyethyleneimine (PEI) as the polymer backbone, which could promote the absorption of interfacial water molecules and allow the hydrogel to adhere strongly to the adherend.<sup>42</sup>

At present, the treatment of the hydration layer is still a key issue in the field of hydrogel underwater adhesion. The two methods of hydrophobicity and water absorption are the common ways to deal with the hydration layer. In addition, researchers are working on designing hydrogels at different molecular levels to treat hydration layers and achieve strong and reversible underwater adhesion.

### 2.2. Covalent bonds

Covalent bonds provide hydrogels with underwater adhesion and cohesion.<sup>22</sup> For substrates with reactive functional groups such as tissue surfaces, underwater adhesion can be achieved by the formation of covalent bonds.<sup>29,38,43,44</sup> The macroscopic integrity can be maintained due to the existence of chemical or physical cross-linking inside the hydrogel, so the hydrogel does not swell excessively and weaken the adhesion when it adheres underwater, while chemical cross-linking is formed by covalent bonds.<sup>38,45,46</sup> Compared with intermolecular forces, covalent bonds are stronger, so the underwater adhesion strength is greater.<sup>47</sup> In this section, the effects of covalent bonds on underwater adhesion and cohesion are discussed, and the formation conditions and influencing factors of covalent bonds are introduced.

Covalent bonds are two or more atoms that use their outer electrons together, and ideally reach a state of electron



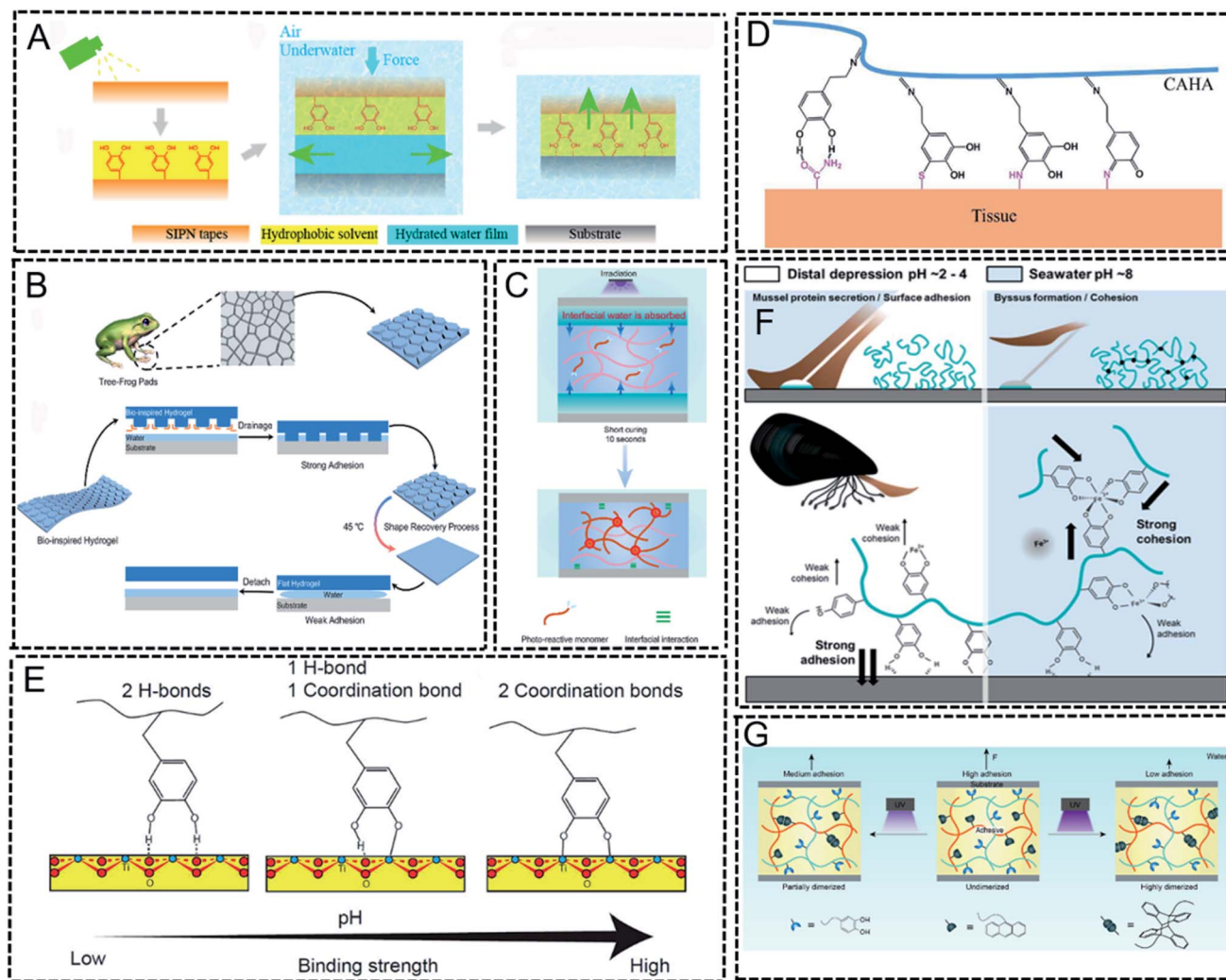


Fig. 1 (A) The repelling of hydration layers by hydrophobic solvents.<sup>34</sup> Figure reproduced with permission from American Chemical Society. (B) Hydrogels with hexagonal microstructures inspired by tree-frog footpads that can repel the hydration layers.<sup>38</sup> Figure reproduced with permission from American Chemical Society. (C) Absorption of the hydration layer by a hygroscopic hydrogel.<sup>41</sup> Figure reproduced with permission from American Chemical Society. (D) Underwater adhesion of hydrogels to biological tissues.<sup>53</sup> Figure reproduced with permission from American Chemical Society. (E) The pH dependence of the binding form of the catechol group to titanium dioxide.<sup>58</sup> Figure reproduced with permission from American Chemical Society. (F) The pH dependent stoichiometry of catechol and Fe<sup>3+</sup> chelation.<sup>61</sup> Figure reproduced with permission from American Chemical Society. (G) Underwater adhesion-tunable hydrogels fabricated on the principle of reversible photo-dimerization of anthracene.<sup>65</sup> Figure reproduced with permission from American Chemical Society.

saturation, thus forming a relatively stable chemical structure. Covalent bonds are stronger than physical interactions, so covalent bonds are often used to improve the underwater adhesion of hydrogels. However, using covalent bonds for underwater adhesion often relies on specific adherend surfaces or requires surface modification.<sup>48,49</sup> The underwater adhesion of hydrogels to biological tissues is usually achieved by covalent bonds.<sup>50–52</sup> Biological tissue surfaces have nucleophiles, including amines, thiol, and hydroxyl groups, and catechol groups (including *o*-quinone groups) in hydrogels can form covalent bonds with nucleophiles on tissue surfaces, thereby adhering to biological tissue (Fig. 1D).<sup>53</sup> Inspired by the adhesion of mussels, various catechol-functionalized underwater adhesion hydrogels have been developed. 3,4-dihydroxy-*l*-

phenylalanine (DOPA) is a catecholic amino acid present in mussel adhesive proteins which can destroy the hydration layer and form covalent bonds with biological tissues to achieve underwater adhesion. Therefore, the catechol moiety of DOPA has been an inspiration for designing underwater adhesion hydrogels.<sup>54,55</sup>

Coordination bonds are a type of covalent bond between hydrogels and metals or metal oxides to achieve underwater adhesion. It is worth noting that coordination bonds are reversible, so the coordination bonds not only maintain the stability of the covalent bond, but also endow the hydrogel with reversible underwater adhesion properties. In addition, the binding of coordination bonds is pH dependent. Taking the catechol group as an example, for a specific metal oxide:

titanium dioxide, at pH  $\sim$  8, the catechol group will form two complexes with the titanium ion. A hydrogen bond and a coordination bond are formed at pH  $\sim$  7 (Fig. 1E).<sup>56–60</sup> Coordination bonds are much stronger than hydrogen bonds, so the underwater adhesion strength of hydrogels can be controlled by adjusting pH. Coordination bonds not only affect the underwater adhesion strength of hydrogels, but also have a certain influence on the cohesion of hydrogels. It is also pH dependent, using the ability of catechol to chelate metal ions, the stoichiometry of catechol and Fe<sup>3+</sup> chelation changes from less to more by adjusting the pH from acidic to weakly alkaline (Fig. 1F).<sup>61,62</sup> This pH-controlled cross-linking degree can indirectly affect the cohesion of the hydrogel, so that the hydrogel can be adjusted to change the mechanical strength according to the actual situation underwater.<sup>56,63,64</sup>

By designing dynamic covalent bonds, the stability of covalent bonds is retained, and reversibility similar to intermolecular forces is obtained. Based on the reversibility of dynamic covalent bonds, researchers have designed a variety of reversible underwater adhesion hydrogels. Since the photodimerization of anthracene is reversible, Wang *et al.* designed a hydrogel with phototunable underwater adhesion, expecting to reversibly tune the underwater adhesion of hydrogels through the reversible binding of dynamic covalent bonds (Fig. 1G).<sup>65</sup> The study showed that although UV-vis spectroscopy detected the recovery of free anthracene groups, the underwater adhesion of the hydrogel did not return to its original value.<sup>65</sup> Therefore, further research is needed to design reversible underwater adhesion hydrogels based on the reversibility of dynamic covalent bonds.

### 2.3. Intermolecular forces

Intermolecular forces include hydrogen bonding, electrostatic interactions, hydrophobic interactions,  $\pi$ - $\pi$  stacking, cation- $\pi$  interactions and metal coordination. The bond energy of a single intermolecular force is weak, but their synergistic effect is crucial for the adhesion properties of hydrogels.<sup>66</sup> The failure and formation of intermolecular forces caused by external forces are reversible. The reversibility of intermolecular forces provides a dissipation mechanism for the hydrogel, which enables the hydrogel to exhibit high toughness, ductility and self-healing properties.<sup>67</sup> A large number of intermolecular forces provide the hydrogel with excellent cohesion.<sup>29</sup> In terms of interfacial adhesion, the reversible nature of intermolecular forces enables the adhesive to have the ability to adhere reversibly.<sup>37</sup> This section will describe the role of intermolecular forces in hydrogel cohesion and interfacial adhesion in underwater adhesion. Table 1 lists the underwater adhesion hydrogels reported in the references at the end of this section, which synergized based on different intermolecular forces to achieve underwater adhesion to different substrates. Before discussing adhesion to different materials, it is necessary to understand the theory that adhesives adhere to materials. Generally, adhesives adhere to materials by two methods: one method is that the adhesive penetrates into the rough surface of the material and forms a “mechanical interlock”. Another method

is through the interaction of the adhesive with the surface of the material. Therefore, when we study the adhesion properties of hydrogels, we should also consider the properties of the surface of the adherend material, such as smoothness and surface energy. As a highly active material, the metal itself easily interacts with the active groups on the surface of the hydrogel, and although the metal surface is relatively smooth, it also adheres more easily.<sup>5</sup> In contrast, glass typically has a lower surface energy, making it easier to release from the mold after fabrication.<sup>68</sup> Therefore, the adhesion strength of the hydrogel to the glass surface is low. Similarly, plastics are also a class of materials with low surface energy,<sup>69,70</sup> especially polytetrafluoroethylene, which adhesives find difficult to adhere to.<sup>74</sup> For wood surfaces, the rough surface provides sites for “mechanical interlocking”, and the reactive groups on the wood surface also make it easy for adhesives to adhere to it.<sup>72</sup> Finally, when considering the adhesion of adhesives to biomaterials, electrostatic interactions can be exploited to form the adhesion because the surfaces of biomaterials are flooded with negative charges.<sup>73</sup> In addition, the necessity of hydrogel application and bioadhesion is to possess good biocompatibility.<sup>5</sup> In conclusion, it is possible to design a strong underwater adhesive hydrogel after fully considering the intermolecular forces of the hydrogel adhesive and the properties of the surface of the adherend material.

**2.3.1. Intermolecular forces in hydrogel cohesion.** The cohesion of underwater adhesion hydrogels can be provided by intermolecular forces synergistically with chemical crosslinks,<sup>74</sup> or by physical crosslinks formed entirely by intermolecular forces.<sup>75,76</sup> The high bond energy of chemical crosslinking provides the hydrogel with certain structural strength, but the covalent bond does not self-heal after breaking. The intermolecular force on the basis of chemical crosslinking can make the crosslinked network of the hydrogel have certain recovery properties. Since the physically crosslinked hydrogels formed by different intermolecular forces are influenced by different environments, smart adhesion can be achieved by adjusting the environment. In the underwater adhesion hydrogel, the synergistic effect of the dominant hydrogen bonding, electrostatic interaction and hydrophobic interaction provides the hydrogel with excellent underwater cohesion. Changing the number of different intermolecular force species can affect the mechanical properties of hydrogels. This subsection will describe the effects of different intermolecular forces and partial synergies on the cohesion of underwater adhesion hydrogels.

General polymer hydrogels contain functional groups such as carboxyl, hydroxyl, and amino groups, which can form a large number of hydrogen bonds to provide cohesion. In addition, the introduction of hydrogen bond donors such as polyoxometalates<sup>77</sup> and catechol groups<sup>78</sup> into the hydrogel can achieve hydrogen bond-dominated physical crosslinking. For example, tungstosilicic acid (SiW) crosslinks hydroxypropyl methylcellulose through hydrogen bonding.<sup>76</sup> Tannic acid crosslinks polyvinyl alcohol through multidentate hydrogen bonds.<sup>78</sup> The hydrogen bond between the catechol-containing polydopamine chain and SiW increases continuously with the increase of solvent polarity to achieve crosslinking.<sup>31</sup> Hydrogen

Table 1 Components, test methods, types of adhesive substrates, adhesive strengths, types of intermolecular forces and application of underwater adhesion hydrogels<sup>a</sup>

| Components                                       | Substrates                         | Test method    | Synergistic force  | Adhesion strength   | Application                                   | Ref. |
|--|------------------------------------|----------------|--|---|---|------|
| P([MATAc][TFSI])                                 | Glass, plastics                    | Lap shear test | Hydrogen bond<br>Electrostatic interaction<br>Hydrophobic interaction<br>Metal coordination<br>Cation- $\pi$ interaction<br>$\pi$ - $\pi$ stacking | Glass $\approx$ 4 MPa<br><br>Plastics $\approx$ 1–2 MPa   | Waterproof transparent tape                   | 100  |
| PMD + PAA  | Glass                              | Lap shear test | Hydrogen bonding<br>Electrostatic interaction<br>Cation- $\pi$ interaction<br>$\pi$ - $\pi$ stacking   | Glass $\approx$ 1 MPa   | Metal-free wet adhesives                      | 82   |
| PAM-Alg-PDA + Ca <sup>2+</sup> /Mg <sup>2+</sup> | Glass                              | Lap shear test | Hydrogen bonding<br>Cation- $\pi$ interaction<br>$\pi$ - $\pi$ stacking  | Glass $\approx$ 150 kPa   | Tissue adhesives                              | 90   |
| OCMC-DA + PAM                                    | Glass                              | Lap shear test | Hydrogen bonding<br>Cation- $\pi$ interaction<br>$\pi$ - $\pi$ stacking  | Glass = 86.3 kPa  | Underwater adhesives                          | 3    |
| PETEA + PEGDA + DA                               | Glass, plastics, wood, ceramic, Fe | Lap shear test | Hydrogen bonding<br>$\pi$ - $\pi$ stacking   | Glass = 205 kPa<br>Plastics $\approx$ 100–300 kPa<br>Wood = 211 kPa<br>Ceramic = 345 kPa<br>Fe = 390 kPa        | Hemostatic sealant                            | 36   |
| P(AA-co-BA-co-Aa)                                | Glass, metal, plastics             | Lap shear test | Hydrogen bond<br>Hydrophobic interaction   | Glass $\approx$ 45 kPa<br>Metal $\approx$ 30–50 kPa<br>Plastics $\approx$ 40–70 kPa                             | Anti-swelling underwater adhesives            | 86   |
| Polydiolcitrate + P(GMA)                         | Glass, metal, plastics, silica     | Lap shear test | Hydrogen bond<br>Hydrophobic interaction   | Glass $\approx$ 80 kPa<br>Metal $\approx$ 50–100 kPa<br>Plastics $\approx$ 50–80 kPa<br>Silica $\approx$ 50 kPa | Tissue sealants and hemostatic dressing       | 95   |
| HPMC + SiW-P(DMAEMA) + Fe <sup>3+</sup>          | Glass, metal, plastics             | Lap shear test | Hydrogen bonding<br>Electrostatic interaction<br>Hydrophobic interaction<br>Metal coordination   | Glass $\approx$ 30 kPa<br>Metal $\approx$ 30 kPa<br>Plastics $\approx$ 20 kPa                                   | Wet and dry adhesives                         | 76   |
| PAM-SDS-C <sub>18</sub> -DA                      | Glass, plastics, wood, tissue      | Lap shear test | Hydrogen bonding<br>Hydrophobic interaction<br>Metal coordination<br>Cation- $\pi$ interaction<br>$\pi$ - $\pi$ stacking                           | Glass $\approx$ 20 kPa<br>Plastics $\approx$ 40 kPa<br>Wood $\approx$ 40 kPa<br>Tissue $\approx$ 50–70 kPa      | Bioadhesives                                  | 94   |
| GE + TP  | Glass, tissue                      | Lap shear test | Hydrogen bonding<br>Cation- $\pi$ interaction<br>$\pi$ - $\pi$ stacking  | Glass = 57.8 kPa<br>Tissue = 152.9 kPa  | Bioadhesive and flexible electronics          | 75   |
| AA + PAANHs + TP + CS + Al <sup>3+</sup>         | Tissue                             | Lap shear test | Hydrogen bonding<br>Electrostatic interaction<br>Cation- $\pi$ interaction<br>$\pi$ - $\pi$ stacking   | Tissue = 23.9 kPa   | Multifunctional specific underwater adhesives | 84   |

Table 1 (Contd.)

| Components   | Substrates  | Test method    | Synergistic force   | Adhesion strength  | Application  | Ref. |
|--|---|----------------|---|--|--|------|
| PAA + CS + TA + Al <sup>3+</sup>                         | Tissue  | Lap shear test | Hydrogen bonding<br>Electrostatic interaction<br>Hydrophobic interaction<br>Cation- $\pi$ interaction<br>$\pi$ - $\pi$ stacking                         | Tissue = 18.1 kPa  | Bioadhesives   | 79   |
| PDAC + PAM + PAA + CS                                    | Tissue  | Lap shear test | Hydrogen bonding<br>Electrostatic interaction<br>Hydrophobic interaction  | Tissue $\approx$ 5 kPa   | Bioadhesives and wearable devices  | 83   |
| P(AAM-co-MAEDS) + P(LMA) + Laponite                      | Plastics, metal   | Lap shear test | Hydrogen bond<br>Electrostatic interaction<br>Hydrophobic interaction   | Plastics $\approx$ 30 kPa<br>Metal $\approx$ 20 kPa  | Antifouling coatings   | 101  |
| OMA-PAM + Alg + PDA + Ca <sup>2+</sup> /Mg <sup>2+</sup> | SS  | Lap shear test | Hydrophobic interaction<br>Hydrogen bonding<br>Electrostatic interaction<br>Metal coordination<br>Cation- $\pi$ interaction<br>$\pi$ - $\pi$ stacking   | SS $\approx$ 120 kPa   | Tissue adhesion, sealing and tissue leakage plugging                                   | 1    |
| P(VGal-co-St) + gallol                                   | Al  | Lap shear test | Hydrogen bonding<br>Metal coordination<br>Cation- $\pi$ interaction<br>$\pi$ - $\pi$ stacking   | Al = 4.09 MPa  | Underwater adhesives   | 102  |
| BA-AA-CABIL-TA   | Al, plastics, ceramic, tissue                             | Lap shear test | Hydrogen bonding<br>Electrostatic interaction   | Al $\approx$ 170 kPa<br>Plastics $\approx$ 100–150 kPa<br>Ceramic $\approx$ 60 kPa<br>Tissue $\approx$ 50 kPa  | Underwater bioelectric monitoring  | 93   |
| SIW + PEG-PPG-PEG  | Glass, plastic, wood                                      | Tack test      | Hydrogen bonding  | Glass $\approx$ 300 kPa<br>Plastic $\approx$ 475 kPa   | Flexible electronic electrode materials  | 81   |
| poly(ATAC-co-PEA)  | Glass <sup>-</sup> , glass <sup>+</sup> , metal, plastics | Tack test      | Hydrophobic interaction<br>Hydrogen bond<br>Electrostatic interaction<br>Hydrophobic interaction<br>Cation- $\pi$ interaction<br>$\pi$ - $\pi$ stacking | Wood $\approx$ 125 kPa<br>Glass <sup>-</sup> $\approx$ 180 kPa<br>Glass <sup>+</sup> $\approx$ 80 kPa<br>Metal $\approx$ 100 kPa<br>Plastics $\approx$ 100 kPa | Underwater transfer, water-based devices, underwater repair and underwater soft robots | 17   |
| P(cation-adj- $\pi$ )                                    | Glass <sup>-</sup> , glass <sup>+</sup> , plastics        | Tack test      | Electrostatic interaction<br>Hydrophobic interaction  | Glass <sup>-</sup> $\approx$ 60 kPa<br>Glass <sup>+</sup> $\approx$ 20 kPa   | Adhesives under physiological or seawater conditions                                   | 13   |
| PAM + C <sub>18</sub> + SDS + Fe <sup>3+</sup>           | Glass, metal, plastic                                     | Tack test      | Hydrogen bond<br>Hydrophobic interaction  | Plastics $\approx$ 50 kPa<br>Glass $\approx$ 20 kPa<br>Metal $\approx$ 10 kPa<br>Plastics $\approx$ 30 kPa   | Soft robots, wearable devices, tissue adhesives and wound dressings                    | 37   |
| VATA (PVA + TA)  | Glass, metal, plastic                                     | Tack test      | Hydrogen bonding<br>Cation- $\pi$ interaction<br>$\pi$ - $\pi$ stacking   | Glass $\approx$ 50 kPa<br>Metal $\approx$ 70 kPa<br>Plastic $\approx$ 70 kPa   | Reusable underwater adhesives  | 78   |

Table 1 (Contd.)

| Components        | Substrates         | Test method  | Synergistic force   | Adhesion strength   | Application   | Ref. |
|-------------------|--------------------|--|---|---|---|------|
| poly(2-EHA-co-AA) | Glass              | Adhesion test                                      | Hydrogen bonding<br>Electrostatic interaction   | Glass $\approx 17 \text{ J m}^{-2}$   | Underwater adhesives  | 98   |
| POMaC + PMMA      | Glass, SS, ceramic | Lap shear test                                     | Hydrogen bonding  | Glass $\approx 1250 \text{ kPa}$<br>SS $\approx 1100 \text{ kPa}$<br>Ceramic $\approx 1200 \text{ kPa}$   | Superglue, tissue sealant, hemostatic dressing and wound dressing | 20   |
| PEGDA + TA        | Tissue             | 90° peel test                                      | Hydrophobic interaction   | Glass $\approx 3500 \text{ J m}^{-2}$<br>SS $\approx 2500 \text{ J m}^{-2}$<br>Ceramic $\approx 2400 \text{ J m}^{-2}$<br>Tissue $\approx 22 \text{ kPa}$ | Wound healing and dressing  | 74   |
| P(AA-co-UCAT)-CS  | Tissue             | Lap shear test<br>180° peel test<br>180° peel test | Hydrophobic interaction<br>Hydrogen bonding<br>Electrostatic interaction<br>Metal coordination<br>Cation- $\pi$ interaction<br>$\pi$ - $\pi$ stacking | Tissue $\approx 9 \text{ kJ m}^{-2}$<br>Tissue $\approx 1200 \text{ J m}^{-2}$  | Biomedical materials, sensors and wearable devices                | 29   |

<sup>a</sup> MATAC: methacryloxyethyltrimethyl ammonium chloride; TFSI: bis(trifluoromethanesulfonimide) lithium salt; PMD: poly(methacryloxyethyl trimethylammonium chloride-random-dopamine methacrylamide); PAA: poly(acrylic acid); PAM: polyacrylamide; PDA: polydopamine; Alg-Na: sodium alginate; OCMC: oxidized carboxymethylcellulose; DA: dopamine; PAM: polyacrylamide; PETEA: pentaerythritol tetraacrylate; PEGDA: poly(ethylene glycol) diacrylate; AA: acrylic acid; BA: butyl acrylate; Aa: acrylated adenine; GMA: glycidyl methacrylate; HPMC: hydroxypropyl methylcellulose; SiW: tungstosilicic acid; P(DMAEMA): poly(dimethylaminoethyl methacrylate); SDS: sodium dodecyl sulfate; C<sub>18</sub>: stearyl methacrylate; GE: gelatin; TP: tea polyphenol; PAANHs: *N*-hydroxysuccinimide ester; CS: chitosan; TA: tannic acid; PDAC: poly(2-acryloyloxyethyltrimethyl ammonium); AAM: acrylamide; MAEDS: [2-(methacryloyloxyethyl)-dimethyl-(3-sulfopropyl); LMA: lauryl methacrylate; OMA: octadecyl methacrylate; VGal: 3,4-dihydroxystyrene; St: styrene; CABIL: choline acrylate bio ionic liquid; PEG-PPG-PEG: poly(ethylene glycol)<sub>10</sub>-*b*-poly(propylene glycol)<sub>65</sub>-*b*-poly(ethylene glycol)<sub>19</sub>; ATAC: 2-(acryloyloxy)ethyl trimethylammonium chloride; PEA: 2-phenoxyethyl acrylate;  $\pi$ : amino acids with aromatic structures; PVA: poly(vinyl alcohol); 2-EHA: 2-ethylhexyl acrylate; POMaC: poly-(octamethylene maleate (anhydride) citrate); PMMA: poly(methyl methacrylate); UCAT: 3-((8,11,13)-pentadeca-trienyl)benzene-1,2-diol; SS: stainless steel.



bonds formed inside the hydrogel will be destroyed by water molecules underwater, resulting in a decrease in cohesion.<sup>79</sup> Therefore, some design strategies need to be applied in underwater adhesion to mitigate the effect of underwater hydrogen bond failure. The underwater cohesion of the hydrogel is ensured by introducing metal cations to coordinate and electrostatically interact with functional groups that can form hydrogen bonds.<sup>80</sup> Su *et al.* introduced  $\text{Al}^{3+}$  into the hydrogel system of polyacrylic acid, chitosan and tannic acid to have

strong electrostatic interaction with acrylic acid and tannic acid, thereby inhibiting the hydrogen bonding between water molecules and acrylic acid and tannic acid.<sup>79</sup> Peng *et al.* introduced the hydrophobic inner core of PEG–PPG–PEG micelles based on the formation of hydrogen-bonded crosslinks by SiW, which provided a second crosslink to strengthen the network. The synergistic effect of hydrogen bonding and hydrophobic interaction effectively strengthens the cohesion of the polymer.<sup>81</sup> This synergy was later used in hydrogels with tannic acid as



Fig. 2 Intermolecular forces in hydrogel cohesion: (A) synergy of hydrogen bonding and hydrophobic interactions between hydrogen bond donors and micelles.<sup>26</sup> Figure reproduced with permission from American Chemical Society. (B) Electrostatic interactions between polymer chains.<sup>83</sup> Figure reproduced with permission from Elsevier. (C) Hydrogen bonding cooperating with electrostatic interactions.<sup>82</sup> Figure reproduced with permission from American Chemical Society. (D) Solvent displacement causing hydrophobic interactions.<sup>86</sup> Figure reproduced with permission from American Chemical Society. (E) Underwater adhesion of dopamine to biological tissues under the synergy of SDS hydrophobicity.<sup>94</sup> Figure reproduced with permission from Elsevier. (F) The intermolecular forces of the hydrophilic groups protected by the hydrophobic chains in the underwater interfacial adhesion.<sup>95</sup> Figure reproduced with permission from American Chemical Society.

a hydrogen bond donor (Fig. 2A).<sup>26</sup> Based on the reversibility of hydrogen bonds, the degree of crosslinking of hydrogels can be regulated to achieve injectable and tunable smart adhesion. For example, urea as a hydrogen bond dissociator (HBD) can dissociate hydrogen bonds, making the hydrogel based on hydrogen bond crosslinking with injectability after dissociation. After injection underwater adhesion, the disrupted hydrogen bond crosslinking in the hydrogel is restored as the HBD diffuses into the underwater environment, and the hydrogel will re-solidify.<sup>75</sup>

Another major intermolecular force is electrostatic interaction. The positive charges in hydrogels that provide electrostatic interactions are derived from cationic functional groups, positively charged chain structures and metal cations, and the negative charges are derived from anionic functional groups.<sup>79,82–84</sup> The electrostatic interaction will not fail due to the influence of the water environment, and the hydrogel based on the intermolecular force-dominated cross-linking has excellent underwater tensile properties. Wang *et al.* synthesized a hydrogel with strong underwater ductility by combining the electrostatic interaction between polyacrylamide, chitosan, 2-acryloxyethyl trimethyl ammonium chloride and polyacrylic acid chain with the hydrophobic interaction of octadecyl acrylate (Fig. 2B),<sup>83</sup> which can still be stretched 54 times after reaching the swelling equilibrium. The synergy of hydrogen bonding and electrostatic interactions provides the most dominant cohesive force in underwater adhesion,<sup>29,79,82</sup> and the amount and ratio of the two intermolecular forces affect the mechanical properties of the hydrogel. Zhang *et al.* synthesized a random copolymer of poly(methacrylateoethyl trimethylammonium chloride-random-dopamine methacrylamide) (PMD), which contained catechol and quaternary ammonium salts. PMD non-covalently crosslinks with poly(acrylic acid) (PAA) chains through hydrogen bonding and electrostatic interactions (Fig. 2C).<sup>82</sup> It is found that the hydrogel has higher tensile properties with the decrease of the PAA ratio, but the toughness and strength decrease, which is related to the decrease of the hydrogen bond ratio.<sup>82</sup>

Benefiting from the conditions of the underwater environment, hydrophobic interactions can exist stably in underwater adhesion. The synergistic effect of hydrophobic interaction was mentioned earlier when introducing hydrogen bonding and electrostatic interaction. Micelles can be formed by long hydrophobic chains in water, which can provide cohesion through physical or chemical interaction of cross-linking polymers.<sup>1,26,81</sup> The hydrophobic regions of micelles contain dynamic and reversible hydrophobic interactions, and the hydrophobic molecular chains in them will rapidly unwind or slip to dissipate energy when disturbed by external forces, resulting in high fracture strength and toughness of the hydrogel.<sup>85</sup> The hydrophobic interaction of the polymer side chain hydrophobic groups caused by solvent replacement increases the cohesion of the hydrogel (Fig. 2D).<sup>86</sup> In addition, the hydrophobic segment endows the hydrogel with a peripheral protective layer that can effectively prevent polymer dispersion. The hydrophobic interaction of the hydrophobic segment and the protective layer

formed on the periphery of the hydrogel make the hydrogel have high anti-swelling properties.<sup>86</sup>

The emergence of  $\pi$ - $\pi$  stacking and cation- $\pi$  interactions often requires the introduction of  $\pi$ -electron-containing groups such as catechol structures<sup>29</sup> and nucleobases<sup>86</sup> into hydrogels. They often cooperate with other intermolecular forces to provide excellent cohesion for the hydrogel. The strength of the cation- $\pi$  interaction inside the hydrogel will affect its cohesion strength, and the strength of the cation- $\pi$  interaction will be affected by the type of cation, the type of aromatic group, and the position of the aromatic group and the cationic group. For example, having cationic groups and aromatic groups in adjacent positions on the same polymer chain has an inverse synergistic effect on the cation- $\pi$  interaction,<sup>87</sup> and the strength of the cation- $\pi$  interaction will weaken with the hydroxylation of aromatic hydrocarbons.<sup>88</sup> However, the hydroxylation of aromatic hydrocarbons in polymer hydrogels can form more hydrogen bonds, so it is necessary to comprehensively consider the effect of different ratios of intermolecular forces on the adhesion properties of hydrogels.

Metal cations can be introduced into the hydrogel to coordinate with the hydrogel network to enhance cohesion. Commonly coordinated metal ions in hydrogels are  $\text{Ca}^{2+}$ ,  $\text{Mg}^{2+}$ ,  $\text{Fe}^{3+}$ , and  $\text{Al}^{3+}$ , and the common functional groups that coordinate with metal ions are carboxyl, hydroxyl, and amino groups. In addition, the coordination form in the hydrogel is also related to the protonation of functional groups. For example, the coordination number of catechol and  $\text{Fe}^{3+}$  changes due to the protonation of the phenolic hydroxyl group affected by pH.<sup>89</sup> There are high contents of  $\text{Ca}^{2+}$  and  $\text{Mg}^{2+}$  in the seawater environment, which can act as coordinating ions in the hydrogel. Liang *et al.* soaked the prepared hydrogel in an artificially simulated seawater environment, and utilized  $\text{Ca}^{2+}$  and  $\text{Mg}^{2+}$  to form coordination with the alginate network, which further strengthened the cohesion of the hydrogel to make it anti-swelling.<sup>90</sup>

**2.3.2. Intermolecular forces in interfacial adhesion.** For interfacial adhesion, the type and properties of the interface substrate will greatly affect the adhesion caused by intermolecular forces. For example, metal coordination often occurs on metal surfaces, hydrophobic interactions occur on the surface of substrates with hydrophobic properties,<sup>37</sup> and  $\pi$ - $\pi$  stacking and cation- $\pi$  interactions often occur on the surface of skin tissue.<sup>29</sup> Most underwater adhesives have broad adhesion properties towards inorganic surfaces. Hydrophobic substances such as oils and fats are contained in skin tissue, but most of the adhesion groups are hydrophilic and cannot adhere well to such hydrophobic surfaces as skin tissue.<sup>91</sup> In addition, in the underwater interfacial adhesion, water molecules will also interact with the adhesion groups to destroy the formation of non-covalent bonds between the hydrogel and the interface, thereby weakening the interfacial adhesion.<sup>36</sup> Inspired by the inclusion of dopamine residues in mussel foot proteins, the excellent adhesion properties of phenolic hydroxyl groups in the catechol structure have been extensively exploited for underwater adhesion.<sup>16,78</sup> However, the existence of the hydration layer seriously affects the intermolecular forces between

catechol and the functional groups at the adhesive interface.<sup>92</sup> Therefore, the precondition for the effective interfacial adhesion provided by the intermolecular force of the underwater adhesive is the ability to remove the hydration layer and to ensure the effective adhesion of hydrophilic groups.

Although the hydrogel will remove the hydration layer to enhance the adhesion to the adherend when it adheres underwater, the hydrogen bond sites that play a role in adhesion will be disturbed by surrounding water molecules over time, resulting in the weakening of interfacial adhesion. In addition, the long-term underwater environment causes swelling effects on the hydrogels, which lead to the failure of their partial cohesion and intermolecular forces at the interface. By observing the law of hydrogel underwater adhesion time and adhesion strength, we found that the interfacial adhesion dominated by hydrogen bonds decreased by more than 50% compared with the highest strength after equilibrium with the increase of time.<sup>75,79,90</sup> But the equilibrium adhesion strength of hydrogels containing hydrophobic groups was only reduced by about 20%.<sup>1,37,93</sup> Therefore, the hydrophobic groups protect the interfacial hydrogen-bonding sites and prevent further swelling of the hydrogel, which ensures the continuous underwater adhesion of the hydrogel that adheres underwater. In the underwater environment, the role of intermolecular forces in interfacial adhesion can be effectively exerted by introducing hydrophobic groups. The hydrophobic groups not only contribute to hydrophobic interactions in the interfacial adhesion of the hydrogel, but also protect the surrounding hydrophilic groups from the binding of water molecules.<sup>20,93</sup> Han *et al.*, using hydrophilic acrylamide and hydrophobic stearic methacrylate (C<sub>18</sub>), sodium dodecyl sulfate (SDS) and Fe<sup>3+</sup>, prepared an underwater adhesion hydrogel with self-regulating function to different substrate surfaces. For hydrophobic surfaces, the hydrophobic layer composed of SDS and C<sub>18</sub> units can directly adhere through hydrophobic interactions. For hydrophilic surfaces, SDS in the hydrogel can self-regulate its hydrophilic end to attach to the hydrophilic surface and convert the surface to hydrophobic properties, thereby enabling adhesion.<sup>37</sup> Pan *et al.* prepared a hydrogel with a hydrophobic layer on the surface by coordinating polydopamine (DA) and SDS with Fe<sup>3+</sup>. DA achieves underwater adhesion to biological tissues through hydrogen bonding,  $\pi$ - $\pi$  stacking, cation- $\pi$  interactions, and hydrophobic interactions under the synergy of SDS hydrophobicity (Fig. 2E).<sup>94</sup> When designing underwater adhesives, it is necessary to select the appropriate size and ratio of hydrophobic groups to achieve optimal adhesion performance.<sup>95,96</sup> Wang *et al.* synthesized different polymers by introducing aliphatic diols with carbon chain lengths of 4, 8, and 12, respectively. Through experiments, it was found that the polymers synthesized from aliphatic diols with a carbon chain length of 8 have the best underwater adhesion properties. Because the long hydrophobic chain in the adhesive provides excellent drainage, it can maximize the protection of the adhesive properties of the hydrophilic group of the adhesive. Additionally, the length of the hydrophobic chain in the polymer network determines the strength of the hydrophobic interaction between the adhesive and the substrate (Fig. 2F).<sup>95</sup>

Intermolecular force-dominated or cooperative adhesion is mainly pH dependent. The increase of pH in the underwater environment will affect the degree of protonation of different functional groups in the hydrogel, which in turn affects the adhesion performance dominated by intermolecular forces. With the increase of basicity, the catechol group easily captures free radicals and oxidizes to quinones, which leads to the failure of the adhesion of the phenolic hydroxyl group as the hydrogen bond donor.<sup>97</sup> Carboxyl groups can mainly form hydrogen bonds and electrostatic interactions, and the ratio of the two intermolecular forces is also related to the protonation of carboxyl groups affected by pH. The increase in pH led to deprotonation of the carboxyl group, which weakened its hydrogen bonding with other functional groups inside the gel or with the adhesive interface, resulting in a decrease in the adhesion performance. In addition, the negatively charged hydrogels caused by deprotonation of the carboxyl group would cause electrostatic repulsion with the negatively charged interface to further affect the adhesion. Although the negative charge of the deprotonated carboxyl group can enhance the electrostatic interaction, the overall adhesion performance of the hydrogel still decreases compared with the contribution of hydrogen bonding to the adhesion.<sup>82,98</sup> Changes in the hydrogel network hydrophilicity and hydrophobicity caused by the protonation of functional groups can also affect the adhesion properties. For example, under acidic conditions, the tertiary amine groups of the poly(dimethylaminoethyl methacrylate) (PDMAEMA) units in the hydrogel are protonated, and the hydrophilic network leads to lower underwater interfacial adhesion. The deprotonation of the tertiary amine groups on the PDMAEMA units with increasing alkalinity leads to enhanced hydrogel network hydrophobicity and thus improved adhesion.<sup>76</sup> pH affects the intermolecular forces of hydrogels by affecting the protonation of different functional groups, which can play a major role in the regulation of underwater adhesion.

Since many solid surfaces are negatively charged, the adhesion of hydrogels to interfaces in aqueous environments is improved by electrostatic interactions, where the adhesion strength can be adjusted by ionic strength.<sup>99</sup> Polyelectrolyte hydrogel adhesives are rich in ionic groups that enable adhesion through electrostatic interactions in aqueous environments. However, some polyelectrolyte hydrogel adhesives are affected by ionic strength in the aqueous environment. Strong interchain attraction will cause the hydrogel to shrink inside, while strong interchain repulsion by the osmotic pressure of the dissociated counterions will cause the hydrogel to swell, both of which lead to poor hydrogel adhesion.<sup>17</sup> In addition to polyelectrolyte hydrogels, the electrostatic interactions that occur during normal adhesion are also affected by the ionic strength, which leads to the effect of hydrogel adhesion in specific environments being affected. In order to avoid the influence of ionic strength, many researchers proposed to use cation- $\pi$  interactions to improve this problem. Gong *et al.* found that copolymers with adjacent cation-aromatic sequences can be synthesized by cation- $\pi$  complex-assisted radical polymerization, and produce strong and reversible adhesion to negatively charged surfaces in seawater.<sup>36</sup> It was also found that the aromatic hydrocarbons on the



copolymers can enhance the electrostatic interaction, even in the solution environment of high ionic strength, which can have high electrostatic interaction, opening a way for the development of adhesives using salt water. Based on the above theory and inspired by the adhesion mechanism of barnacles, the research group prepared a cationic and aromatic monomer hydrogel with aromatic composition.<sup>17</sup> Due to the interchain  $\pi$ - $\pi$  and cation- $\pi$  interactions, hydrogels can adhere to different surfaces *via* interfacial electrostatic and hydrophobic interactions in an aqueous environment. Although the ionic strength in the solution environment will affect the strength of electrostatic interaction, with the continuous discovery and in-depth research of researchers, there will be more and more other methods to improve it in the future.

### 3. Design strategies for underwater adhesion hydrogels

According to the bonding method, various types of underwater adhesion hydrogels developed in the last decade can be broadly classified into gel-type hydrogels and sol-type hydrogels. Gel-type hydrogels are elastic semisolids with a certain morphology that can adhere directly to wet surfaces through molecular interactions.<sup>103</sup> However, their adhesion underwater is generally low due to adhesion interface drainage and poor interfacial contact problems. In contrast, sol-type hydrogels, as a liquid underwater adhesive, have strong underwater adhesion due to good fluidity and interfacial contact.<sup>17,47</sup> However, conventional sol-type hydrogels have long curing times, and are difficult to separate as needed for reversible bonding. Therefore, the development of sol-type hydrogels focuses on the reduction of curing time and reversible adhesion problems, while the design of gel-type hydrogels focuses on hydration layer removal and formation of effective contact surfaces.

Based on the presented underwater adhesion mechanisms, the design strategy of the underwater adhesion hydrogel will be a hydrogel designed through these adhesion mechanisms. These adhesion mechanisms will interact to play a complementary, additive or even multiplicative role. That is, the adhesion mechanisms need to be able to complement each other's functions, overcome shortcomings, and prevent failure. However, in order to obtain optimal performance, the underwater adhesion strategy must be designed to match the properties of the underwater environment in which it is to be applied, while meeting the requirements of the mechanical properties of the underwater application.

#### 3.1. Gel-type hydrogels

Gel-type hydrogels are soft solids with a certain morphology that can adhere directly to moist surfaces through molecular interactions. This type of adhesive usually exhibits transient and reversible adhesion. However, hydrogels based on single molecular interactions usually have a weak adhesion strength (50 kPa).<sup>21</sup> This is due to the fact that the non-covalent interactions at the interface are greatly weakened by the formation of a hydrated layer. Due to the hydrophilic nature of polymers and

the presence of highly swollen networks in hydrogels,<sup>21</sup> it is difficult to obtain strong adhesion properties of hydrogels underwater. Water molecules can form a hydration layer on the hydrogel surface or penetrate into the internal network of the hydrogel, leading to the detachment of the adhesive layer and the hydrolysis of the hydrogel polymer network.<sup>49</sup> In the adhesion mechanism, we summarized in detail the methods for removing the hydration layer. Among them, at the molecular level, hydrophobic interactions are constructed by introducing hydrophobic monomers or solvents<sup>1,34,104</sup> to provide a basis for underwater adhesion (Section 2.1.1). Then, synergizing with other non-covalent interactions<sup>76</sup> is a general design strategy for underwater adhesion hydrogels. Hydrophobic interactions play an important role in regulating the adhesion and cohesion of the adhesion system (Section 2.3).<sup>105</sup> For example, Wang *et al.* successfully synthesized conductive gel electrodes based on bioionic liquids by polymerization of hydrophilic acrylate and hydrophobic butyl acrylate in an organic solvent (DMSO).<sup>93</sup> The hydrophobic aggregation induced by solvent exchange imparts durable underwater adhesion and swelling resistance to the gel. During the solvent exchange process, water diffuses into the organogel and replaces DMSO, leading to the aggregation of hydrophobic segments in the gel and enhancing the cohesion of the gel network. Cui *et al.* combined macroscopic surface modifications and hydrogels with dynamic bonds to modulate the arrangement of supramolecular functional groups in dynamic hydrogels on the surface of the hydrogel, thus enabling rapid hydrophobic interactions to occur with the surface of the substrate.<sup>37</sup> Thus, the hydrogel is successfully endowed with rapid and reversible strong adhesion underwater. Moreover, the poor mechanical properties and lack of functionalization of conventional hydrogels for underwater applications can be solved by introducing other non-covalent interactions to extend the application areas of hydrogels in underwater applications. For example, Liu *et al.* reported an underwater adhesion gel based on the synergy of hydrophobic interaction and hydrogen bonding adhesion.<sup>86</sup> The gel was formed by the copolymerization of hydrophobic and hydrophilic monomers and nucleobases with adhesion factors in dimethyl sulfoxide (DMSO) solvent. The underwater adhesive behavior based on the strategy of solvent exchange induced hydrophobic aggregation confers fast bonding to the hydrogel. The strong mechanical properties of the bonding material are a prerequisite for practical applications. The hydrophobic interaction and reversible hydrogen bonding synergistically cross-link (Fig. 3A-C)<sup>74,93,106</sup> the energy dissipation mechanism of the gel, endowing the hydrogel with outstanding self-recovery properties and fatigue resistance, greatly extending its application in underwater environments. Similarly, in marine environments with high ionic concentrations, electrostatic interactions are usually introduced to cross-link synergistically with hydrophobic interactions to form gels with strong underwater adhesion (Fig. 3D-F).<sup>13,104,107</sup> This type of hydrogel is usually inspired by proteins containing amino acids secreted by marine organisms and consists of cations and aromatic sequences. Due to the strong  $\pi$ - $\pi$  and cation- $\pi$  interactions, both cationic and aromatic groups play an important role in the cohesion and

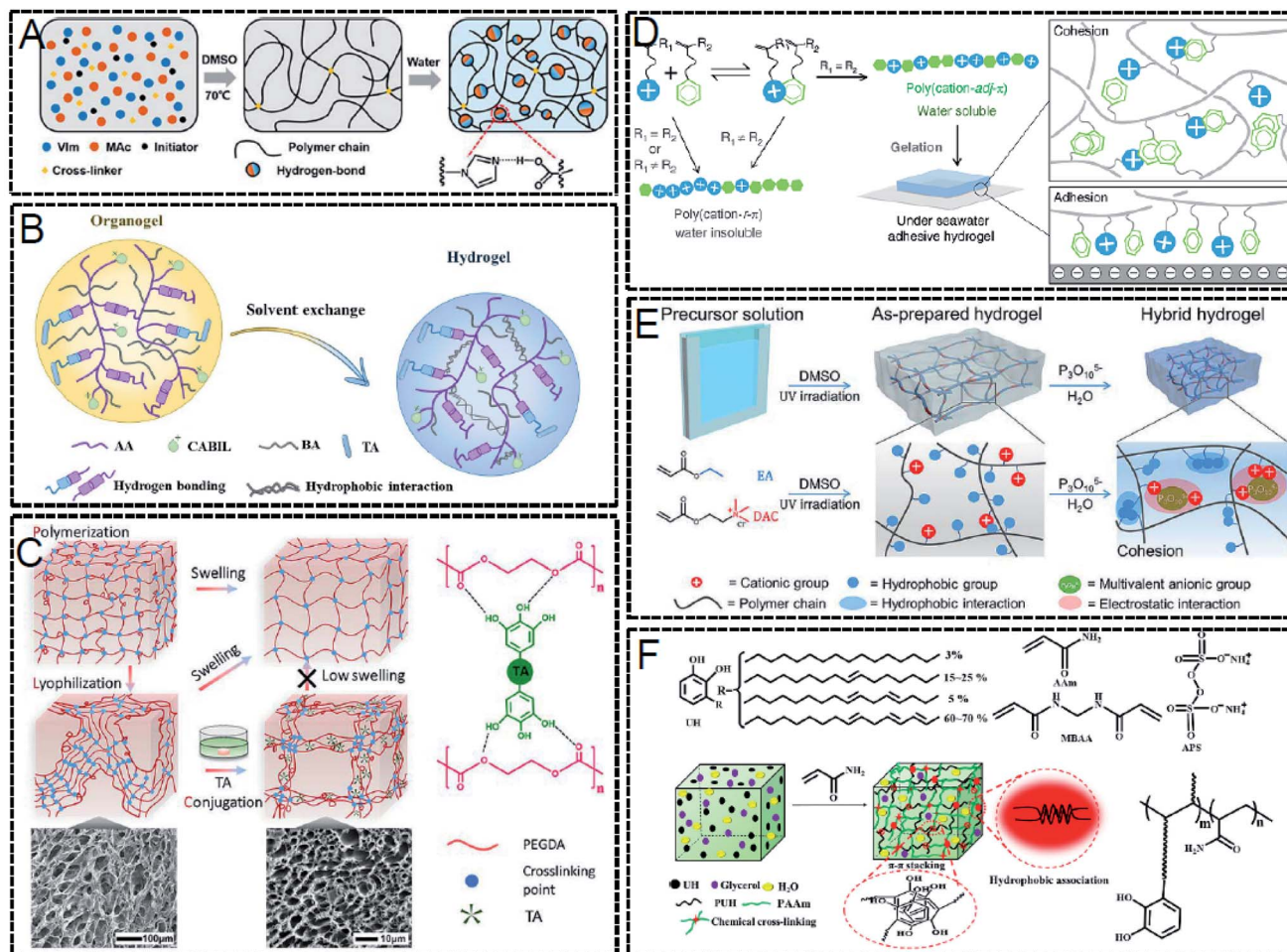


Fig. 3 (A) Tough P(VI-co-MAAc) hydrogels constructed by solvent exchange to enhance intergroup hydrogen bonding forces.<sup>106</sup> Figure reproduced with permission from American Chemical Society. (B) BACT gels constructed by copolymerization of hydrophilic and hydrophobic monomers in organic solvents.<sup>93</sup> Figure reproduced with permission from Elsevier. (C) PEGDA/TA hydrogels constructed by reversible cross-linking of tannic acid introduced in the covalent network.<sup>74</sup> Figure reproduced with permission from American Chemical Society. (D) Underwater adhesion hydrogels with an adjacent cationic-aromatic sequence.<sup>13</sup> Figure reproduced with permission from Springer Nature. (E) Formation of hybrid poly(EA-co-DAC)/STPP hydrophobic hydrogels *via* electrolyte monomer-assisted copolymerization and ionic cross-linking.<sup>107</sup> Figure reproduced with permission from American Chemical Society. (F) PAAm-co-PUH hydrogels with hydrophobic linkage and  $\pi$ - $\pi$  interactions provided by catechol moieties.<sup>104</sup> Figure reproduced with permission from American Chemical Society.

adhesion of hydrogels. With the help of neighboring aromatic groups that break the water layer, electrostatic interactions can provide strong interfacial adhesion in water. In addition, this type of hydrogel has excellent mechanical strength and toughness due to the dynamic  $\pi$ - $\pi$  and cation- $\pi$  cross-linking between the chains.<sup>13</sup> In conclusion, hydrophobic interactions provide the basis for underwater adhesion to form good interfacial adhesion and rapid formation of non-covalent interactions at the adhesion interface. Adhesion based on synergistic interactions between weak interaction types of hydrogels is usually fast and reversible. Furthermore, the synergy between different adhesion interactions confers different functionalization of the hydrogels for applications in underwater environments.

In nature, many organisms are able to adapt to complex water environments by developing micro/nanostructures with unique functions, for example, the setae of gecko feet, the foot

pads of tree frogs, the hexagonal microstructures of clingfish, *etc.* (Fig. 4). Biomimetic microstructures for rapid drainage at the microscopic scale provide an alternative idea for design strategies of underwater adhesion hydrogels (Section 2.1.1).<sup>38,39,108-114</sup> Inspired by these bioadhesive properties and structures, many underwater adhesion hydrogels have been reported. Inspired by the adhesive disc of the clingfish, Rao *et al.* obtained hydrogels with fast, strong and reversible underwater adhesion by combining polyamphiphilic electrolyte hydrogels with dynamic ionic bonding and biomimetic surface drainage structures.<sup>39</sup> The hexagonal surface grooves can be used as a fast drainage channel during underwater contact. Meanwhile, the multi-amphiphilic hydrogel can form reversible ionic bonds with charged surfaces (positively or negatively charged surfaces) and form interfacial bridges with ionic bonds in the body to effectively dissipate energy during deformation. Therefore, multi-amphiphilic electrolyte hydrogels based on the



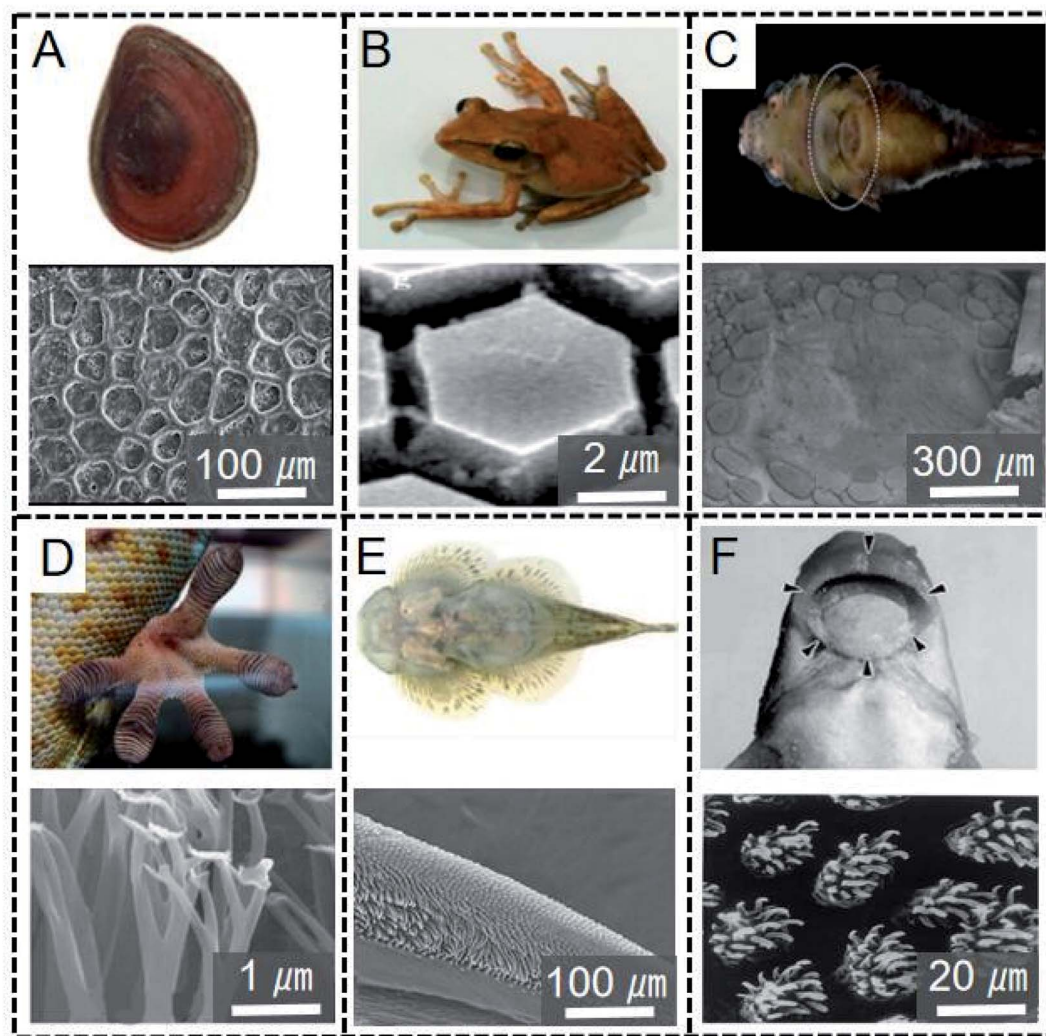


**Fig. 4** Fine structure of typical organisms in nature with special micro/nanostructures and their functional units. (A) The microporous structure of the inner surface of snails giving them a strong adhesion to human tissues.<sup>115</sup> Figure reproduced with permission from American Chemical Society. (B) Tree frogs flexibly climbing on wet surfaces because their toe pads have protruding epithelial keratinocytes.<sup>116</sup> Figure reproduced with permission from American Chemical Society. (C) Clingfish characterized by ventral annual star discs covered with papillae for underwater attachment.<sup>115</sup> Figure reproduced with permission from American Chemical Society. (D) Geckos relying on specific nanostructures on foot hairs and van der Waals interactions between foot scrapers and substrate surfaces to produce anisotropic adhesion, resulting in switchable adhesion behavior.<sup>117</sup> Figure reproduced with permission from Elsevier. (E) Loaches using their pectoral and pelvic fins with needle-like setae to form the suction system.<sup>118</sup> Figure reproduced with permission from Elsevier. (F) Tubercles bearing hooks on the jaw sheaths of teleosts that may assist in mechanical interlocking with the substrates.<sup>119</sup> Figure reproduced with permission from Elsevier.

synergistic effect of both bionic microstructural surface engineering and molecular interactions are able to rapidly and reversibly attach to negatively and positively charged substrates in water.

In addition to strong adhesion properties, many organisms are able to accurately control and switch their adhesion strength. Geckos rely on specific nanostructures on foot hairs and van der Waals interactions between foot scrapers and substrate surfaces to produce anisotropic adhesion, resulting in switchable adhesion behavior.<sup>110,114</sup> The octopus relies on tentacle muscles to control the structural deformation of the suckers to regulate the pressure between the inside and outside of the suckers, thus controlling the adhesion strength of the

suckers.<sup>108,109</sup> Achieving switchable adhesion underwater by mimicking biologically controlled microstructures is a good strategy. However, mimicking these microstructures is still a major challenge because most organisms can control the microstructure changes by inherent muscle contractions or secrete some chemically complex substances to control the switchable adhesion properties. The advantage of this microstructure bonding system is that it can be bonded repeatedly without chemical reactions and chemical residues. The adhesion can also be quickly adjusted by controlling the changes in microstructure. Inspired by this, Zhang *et al.* combined temperature-controlled shape memory hydrogels with a surface structure imitating a tree frog footpad, which facilitated the

principle of rapid drainage of hexagonal microstructures to enhance wet adhesion.<sup>38</sup> Based on the shape memory effect, the microstructures were immobilized to the surface of the hydrogel. The temperature-controlled surface microstructure enables reciprocal changes from hexagonal drainage structures to planar structures, resulting in switchable underwater adhesion, which is an ideal and indispensable material in many fields. In addition, the dual physical effects of weak hydrogen bonding and dipole–dipole interactions can significantly improve the mechanical properties of hydrogels. Due to the presence of a large number of hydrogen bonds and dipole–dipole interactions in the hydrogel, an obvious hysteresis loop is formed, which can effectively dissipate energy, and the hydrogels have high tensile toughness and self-recovery properties. The strategy based on bionic microstructure surface engineering and dynamic bonding is versatile and flexible, and can be extended to other combinations of surface design materials.

In summary, due to the poor interfacial contact of gel-based hydrogels, the bond strength of gel-based hydrogel adhesives is generally weaker than that of sol-type hydrogel underwater adhesives. For gel-type hydrogels based on weak interaction synergies, removal of the hydrated layer remains a major challenge. Although the synergy of hydrophobic and other weak interactions achieves a certain degree of dehydration at the molecular level, efficient drainage of interfacial water at the macroscopic level remains a challenge. The synergistic effect based on the combination of bionic microstructure surface engineering and dynamic adhesive toughness hydrogel can achieve efficient drainage at the microscopic level while retarding the crack expansion during peeling. This allows for effective energy dissipation and fast, strong, and reversible adhesion underwater. This strategy will be an effective way to improve the adhesion performance underwater in the future.

### 3.2. Sol-type hydrogels

Sol-type hydrogels are formed by curing a liquid precursor solution underwater, where interfacial interactions at the molecular level occur.<sup>21</sup> Subsequently, the liquid is polymerized or cross-linked to form a solid. Sol-type hydrogels generally have high adhesive strength due to sufficient contact at the molecular level and strong mechanical interlocking, and usually fail cohesively, indicating that the adhesive strength is much greater than the cohesive strength.<sup>47,103</sup> However, they require long curing times compared to gel-type hydrogels and the bonding is usually irreversible.<sup>21</sup> Therefore, the design of sol-type hydrogel adhesives focuses on shortening the curing time and forming reversible adhesions that ensure excellent cohesion underwater. Below we have summarized the design issues for sol-type hydrogel curing structures and design strategies for reversible adhesion, respectively.

Widely used cyanoacrylate adhesives exhibit strong adhesion in air, but when used in an aqueous environment, they harden rapidly, forming a hard plastic layer that eventually leads to loss of adhesion.<sup>120,121</sup> Although commercially available epoxy resins<sup>122</sup> and polyurethanes<sup>123</sup> exhibit strong underwater adhesion, they usually require a long curing time. A growing number

of studies on marine organisms capable of secreting adhesion substances such as mussels, sandbag worms, barnacles, *etc.* suggest that liquid curing plays a key role in achieving underwater adhesion.<sup>42</sup> In a few cases, special means (*e.g.*, heat,<sup>124</sup> UV radiation,<sup>22,125</sup> solvent exchange<sup>104</sup> and strong oxidants<sup>105</sup>) may help to achieve relatively stable gelation of liquid hydrogels. However, they may be greatly limited in their applicability due to their additional cytotoxicity. Cui *et al.* designed and synthesized a catechol side-branched hyperbranched polymer gel (HBPA) with a hydrophobic backbone and a hydrophilic adhesive triggered by water for rapid curing using the mechanism of hydrophobic interaction to induce spontaneous curing cross-linking of the adhesive.<sup>36</sup> When the binder comes into contact with water, the hydrophobic chains rapidly aggregate to form co-permeates that replace the water molecules on the adherent surface, triggering increased exposure of the catechol moiety and rapid curing underwater to achieve strong adhesion. In addition, HBPA exhibits reproducible and durable underwater adhesion. Despite the facilitative effect of catechols on underwater adhesion, the synthesis of catechol-containing polymers is difficult to scale up and involves complex functionalization and/or protection treatments because the catechol moieties are prone to autoxidation.<sup>106,126,127</sup> Zhao *et al.* proposed an aqueous and catechol-free strategy to prepare robust underwater adhesives by using biomass pulping residues lignosulfonate (LS) and the economic industrial additive polyamide amine-epichlorohydrin (PAE-Cl) to prepare robust underwater adhesives (Fig. 5A).<sup>128</sup> The mixing of LS and PAE-Cl solutions, electrostatic complexation and hydrophilic stabilization act synergistically to induce fluid but water-insoluble adhesives. The LS-PAE adhesives allow immediate adhesion to various substrates underwater and undergo spontaneous curing, thus significantly improving underwater adhesion.

Accelerating the formation of polymers by activating the cross-linking reaction of hydrogels or using the hydration process to form nanocrystals to shorten the curing time provides another idea for the design of sol-type hydrogels.<sup>75</sup> Wan *et al.* synthesized hydrogels with isocyanate-terminated polypropylene glycol (PPG) and isocyanate-terminated dopamine bis(hydroxymethyl)propionate (DBHP).<sup>42</sup> When the hydrogel is applied underwater, the amino formed by the reaction of the isocyanate group with water rapidly reacts with other isocyanate groups to accelerate the cure. Meanwhile, the bidentate hydrogen bond formed by the catechol group and  $\pi$ - $\pi$  interaction are stronger than those of water to achieve strong adhesion.<sup>33,129</sup> Due to the polyurethane group's ability to generate a strong hydrogen domain, the negative effect of improving the dispersion of water molecules is improved.<sup>130</sup> Jia *et al.* brought in a polyurethane structure to help the adhesive eliminate interface water resistance and enhance adhesion. The free radical polymerization of olefin groups was introduced into the PU matrix for covalent cross-linking, which greatly shortened the curing time.<sup>114</sup> A combination of covalent cross-linking, hydrogen bonding and other physical interactions is an effective way to develop strong underwater adhesives. Huang *et al.* developed a PDMS-based adhesive by combining covalent cross-linking with hydrogen bonding and other physical

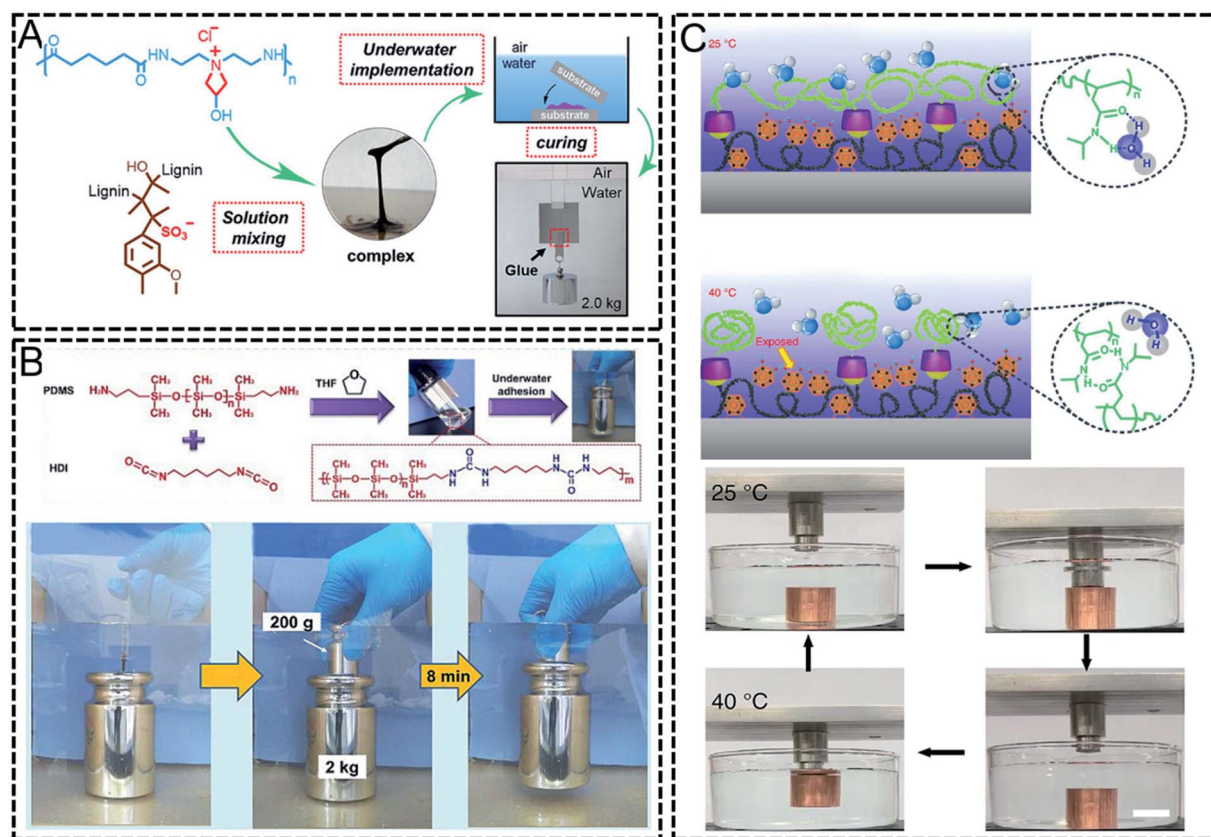


Fig. 5 (A) Catechol-free LS-PAE adhesive with high underwater adhesion achieved by synergistic electrostatic complexation and hydrophilic stabilization.<sup>128</sup> Figure reproduced with permission from American Chemical Society. (B) Fully cured HDI-PDMS adhesive in water based on chemical cross-linking and hydrogen bonding interactions, and a schematic of its curing in water for 8 min load-bearing.<sup>131</sup> Figure reproduced with permission from Elsevier. (C) Schematic of the screening and recovery of the interfacial interaction of DOPA under different temperatures.<sup>133</sup> Figure reproduced with permission from Springer Nature.

interactions.<sup>131</sup> The adhesive can be fully cured under aqueous conditions and has strong underwater adhesion to various substrates. After curing for 8 minutes, a weight (2 kg) can be easily lifted (Fig. 5B)<sup>131</sup> with an adhesion strength greater than 47 kPa. Inorganic fillers can also be added, and polymer chains within the gel are attached to the nanoparticles produced by the hydration process, acting as a bridge between the polymer chains and promoting cross-linking.<sup>132</sup> Zhang *et al.* mixed acrylamide, *N,N*-methylene acrylamide and inorganic filler to form a nano-composite polyacrylamide (PAM) hydrogel precursor. The nanocrystals generated by the inorganic fillers through a rapid hydration process act as physical crosslinking agents to accelerate gel curing.<sup>40</sup>

In addition to rapid curing for strong adhesion in an aqueous environment, adhesive materials that can adhere to target properties on demand are highly desirable in many practical applications. Therefore, one of the great challenges in adhesion science and technology is the development of smart materials with reversible adhesion properties in an aqueous environment. But most of the reversible adhesion designs have focused only on gel-type hydrogels based on molecular interactions. This is because semi-solid gels can rely on switching the interfacial interactions between the functional groups of the

adhering surface and the solid surface to control reversible underwater adhesion. However, gels often require laborious pre-modification due to low adhesion strength.<sup>133</sup> As another important form of underwater adhesive, liquid adhesives have attracted a lot of attention due to their high adhesion strength, desirable flowability and wide applicability.<sup>21</sup> Therefore, many researchers have worked on the problem of irreversible adhesion of sol-type hydrogels with excellent cohesive strength. Researchers have greatly improved this problem by exploiting the dynamic cross-linking of chemical bonds due to the external environment of the hydrogel (temperature,<sup>124</sup> light,<sup>22,114</sup> *etc.*) and the interaction between the hydrogel and the interface. Zhao *et al.* exploited the interaction of host-guest molecules and the adhesive properties of catechol chemistry, as well as reactive polymers, to screen and activate interfacial interactions on demand by local temperature triggering only.<sup>133</sup> Modulation of the interfacial interactions is reversibly activated by a simple temperature trigger (Fig. 5C).<sup>133</sup> The adhesion in this adhesive can be dynamically regulated in a more flexible and faster manner than if it were controlled by multiple external stimuli.

Accelerating the formation of polymers by activating cross-linking reactions in hydrogels provides another idea for the design of sol-type hydrogels. One isocyanate group in



polyurethane can react rapidly with water to form an amino group, which subsequently reacts with another isocyanate group to form a polymeric or cross-linked structure. Xia *et al.* proposed a simple and powerful strategy for rapid curing of mussel underwater adhesives by exploiting the strong underwater adhesion of catechol groups in mussel adhesion proteins (MAPs) and the fast curing ability of polyurethane (PU) prepolymers.<sup>33</sup> They prepared a mussel PU prepolymer consisting of isocyanate-terminated polypropylene glycol (PPG) and isocyanate-terminated dopamine bis(hydroxymethyl)propane (DBHP). When it is applied for underwater bonding, the isocyanate group can react with water at the interface to form a polymer structure. At the same time, the surface can be easily immobilized by catechol groups. As a result, fast and strong adhesion can be achieved. An average underwater adhesive strength of about 1.2 MPa was obtained on the glass substrate under underwater conditions with a curing time of only about 30 s. In addition, no organic solvents or cross-linking reagents are required in this adhesive, which is certainly an advantage in practice. This fast and strong underwater curing property is superior to the bonding properties of many other reported mussel-inspired adhesives. At the same time the underwater curing process of PUP-PPG-DBHP shows good tolerance to pH, ionic strength and temperature variations. This adhesive opens an innovative and convenient way towards a viable solution in the field of underwater engineering.

To sum up, sol-type hydrogels can achieve high underwater adhesion at present, but most gel curing still takes several hours, which greatly limits practical application. The rapid reaction of polymerization or crosslinking of groups not only strengthens cohesion and establishes strong interface adhesion, but also realizes accelerated curing, making curing time controlled in a few seconds or minutes possible. The dynamic cross-linking of chemical bonds and the interaction between the interface and the gel provide a solution for the realization of reversible adhesion. Various design strategies provide feasible solutions for improving the performance of hydrogels.

## 4. Methods of testing hydrogel underwater adhesion

Testing the underwater adhesion of hydrogels is the most basic way to characterize the underwater adhesion properties of hydrogels. The test method for adhesion of hydrogels in a dry environment is also applicable to underwater adhesion. When testing the underwater adhesion, the hydrogel and the adherend are firstly bonded underwater. The adhesion of hydrogels is usually characterized in two ways: adhesion strength and adhesion toughness. Adhesion strength is the maximum force per unit area, while adhesive toughness is the energy required to separate the hydrogel per unit area from the adherend.<sup>66</sup> It has been reported that the lap shear, tack test and adhesion test can measure the adhesion strength, while the peel test and tensile test can characterize the adhesion toughness, and the five test methods for the underwater adhesion of hydrogels will be described in the following sections.<sup>129</sup>

The lap shear test is a common method for evaluating the adhesion strength of hydrogels to adherends underwater. In the lap shear test, a portion of the area of the two adherends overlaps and can be bonded together by the hydrogel. After the hydrogel adheres to the adherend underwater, the adhesion strength can be tested using a universal testing machine in a dry environment. The test specimens are pulled apart by an applied external force in a direction parallel to the overlapping area, resulting in the maximum force required for separation, thus the adhesion strength is equal to the maximum force per unit contact area (Fig. 6A).<sup>21</sup> Tack test is another method to characterize the underwater adhesion strength of hydrogels, by which the hydrogel is immobilized on the top of the sensor or on a substrate in water. By applying a certain external force, the sensor is bonded to the adherend fixed underwater, after which the sensor is retracted until the hydrogel and the adherend are completely detached. The sensor can generate the maximum force required to retract during the retraction process, and the adhesion strength is equal to the maximum force required to retract a unit area of hydrogel (Fig. 6B).<sup>43</sup> The texture analyzer can measure the adhesion strength of the hydrogel through the adhesion test (Fig. 6C). The adhesion test is similar to the tack test, while the difference is that the adhesion test fixes the hydrogel on the chassis of the texture analyzer and the adhesion strength is characterized by testing the adhesion of the hydrogel to the spherical probe. The adhesion energy ( $W_{adh}$ ) can also be calculated from the adhesion strength by both the tack test and adhesion test.<sup>86</sup>

The peel test is a common method to test the adhesion toughness of hydrogels, which can be used to detect the energy required for the hydrogel to peel off per unit width on the contact surface. In the peeling measurement, the hydrogel and the adherend are bonded underwater and then the hydrogel is peeled off on the object at a certain angle ( $90^\circ$  or  $180^\circ$ ) by applying an external force (Fig. 6D). The peel force gradually increases at the beginning until the applied energy is greater than the adhesion toughness of the hydrogel, which can be used to obtain the average peel force of the hydrogel from the adherend with the reached stable state.<sup>134</sup> When peeling off highly stretchable hydrogels, a backing layer can be used for peeling together with the hydrogel to prevent the hydrogel from breaking during the peeling process, which can limit the stretchability of the hydrogel.<sup>129</sup> For highly stretchable hydrogels, when the external force exceeds its own reversible stretching range, the hydrogel can be damaged and thus affect the accuracy of the test. The unique feature of the tensile test is that the adhesion toughness of the hydrogel can be tested without any external force being applied to the hydrogel. The hydrogel adheres to a substrate with good ductility is lifted at one end (Fig. 6E). When the substrate is stretched by an external force, the hydrogel gradually falls off from the substrate, from which the energy release rate ( $G$ ) can be obtained by calculating the test data.<sup>135</sup>

The above five methods are commonly used to test the underwater adhesion of hydrogels, but these five methods are usually contradictory; for example, the adhesion strength and adhesion toughness are not proportional. Each method has

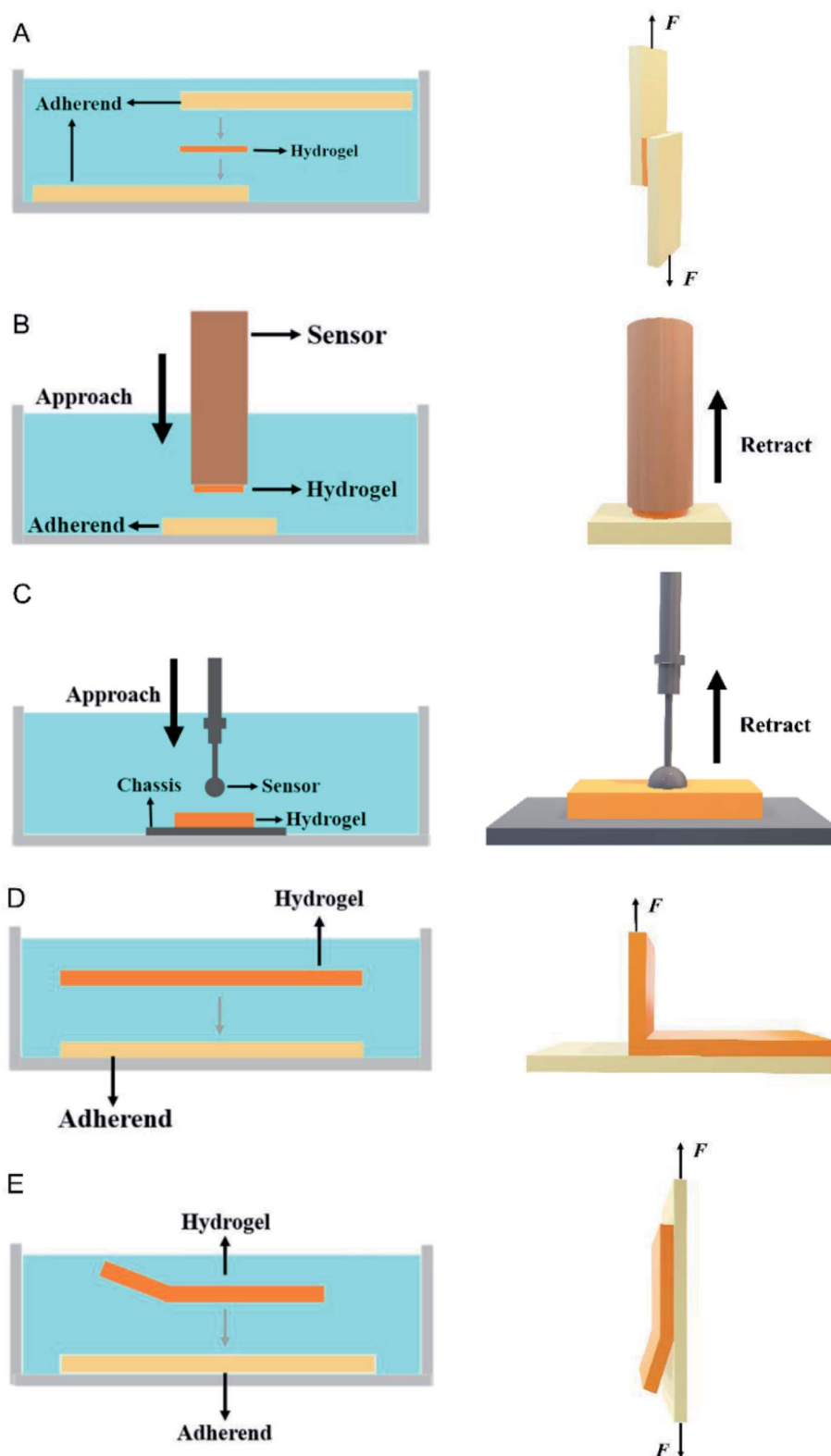


Fig. 6 Methods of testing hydrogel underwater adhesion: (A) lap shear test, (B) tack test, (C) adhesion test, (D) peel test and (E) tensile test.

different requirements for hydrogels; for instance, the lap shear test and tack test are more suitable for sol-type hydrogels, while the adhesion test, peel test and tensile test are more suitable for gel-type hydrogels. In addition, each method will cause artificial

experimental errors to the hydrogel during the actual operation, which will affect the experimental data. Therefore, the development of more sensitive and more objective experimental methods still needs to be explored.



## 5. Applications of underwater adhesion hydrogels

In-depth research on the adhesion mechanism and design strategies of underwater adhesion hydrogels has led to the development and practical application of various underwater adhesion hydrogels (Fig. 7). This section focuses on the applications of underwater adhesion hydrogels in various fields.

### 5.1. Underwater adhesives

Adhesives are widely used in modern society, but with the development of environmental engineering and industrial engineering, underwater adhesives have become indispensable and important materials.<sup>86,136</sup> Because water will affect the internal cross-linking of the gel during underwater adhesion,<sup>33,137</sup> and the hydration layer will destroy the interaction between the hydrogel and the substrate surface, influence of adhesive adhesion.<sup>32,138–140</sup> Due to the hydrophilicity of traditional adhesives, they only maintain weak adhesion underwater, and even lose adhesion. The excellent properties of the new hydrogels, such as strong and durable self-healing, provide a feasible solution for the problem of underwater adhesion, and solve the problem of underwater repair that has long been an issue. In this section, the achievements of underwater adhesives in the fields of underwater engineering and underwater repair are summarized.

In the construction of underwater engineering and water-based equipment, it is inevitable to rely on adhesives to bond the structure and parts (Fig. 8A and B).<sup>78,141</sup> Once the structure and function of underwater adhesives are damaged,

inestimable losses will be caused. Underwater adhesives play an irreplaceable role in underwater engineering because of their strong adhesion to wood and metal structures.<sup>142</sup> Underwater adhesion engineering requires underwater adhesives with high adhesion to ensure long-term effective adhesion. Therefore, in order to meet the needs of underwater adhesion engineering, researchers prepared a variety of high-adhesion underwater adhesives based on the adhesion mechanism of marine mussels.<sup>16,55,84,143–145</sup> When applied underwater, the catechol-styrene hydrogel developed by North *et al.* showed the best adhesion force of about 3 MPa on an aluminum substrate, and the excellent adhesion performance on wood, polytetrafluoroethylene and other materials was far superior to many glues on the market at present.<sup>16</sup> The nanocomposite underwater adhesive developed by Pan *et al.* improved the adhesive adhesion on glass and wood, which could reach more than 1 MPa.<sup>40</sup> With the strong underwater adhesion of the underwater adhesive to the substrate, the normal use of underwater engineering and underwater equipment can be guaranteed.

The lasting stability of an adhesive becomes an important prerequisite for the application of underwater adhesives in underwater engineering. When actually applied to underwater engineering, the ability of an underwater adhesive to effectively repel the hydration layer is the premise of achieving durable and stable adhesion (Section 2.1.). In addition, ensuring that the adhesive will not reduce adhesion due to swelling in water is the key to achieving a durable and stable adhesion. This helps maintain excellent mechanical properties in underwater environments for long periods of time.<sup>17</sup> Due to the complex underwater environment, the adhesive defect is inevitably caused, which leads to the decrease of adhesive force in

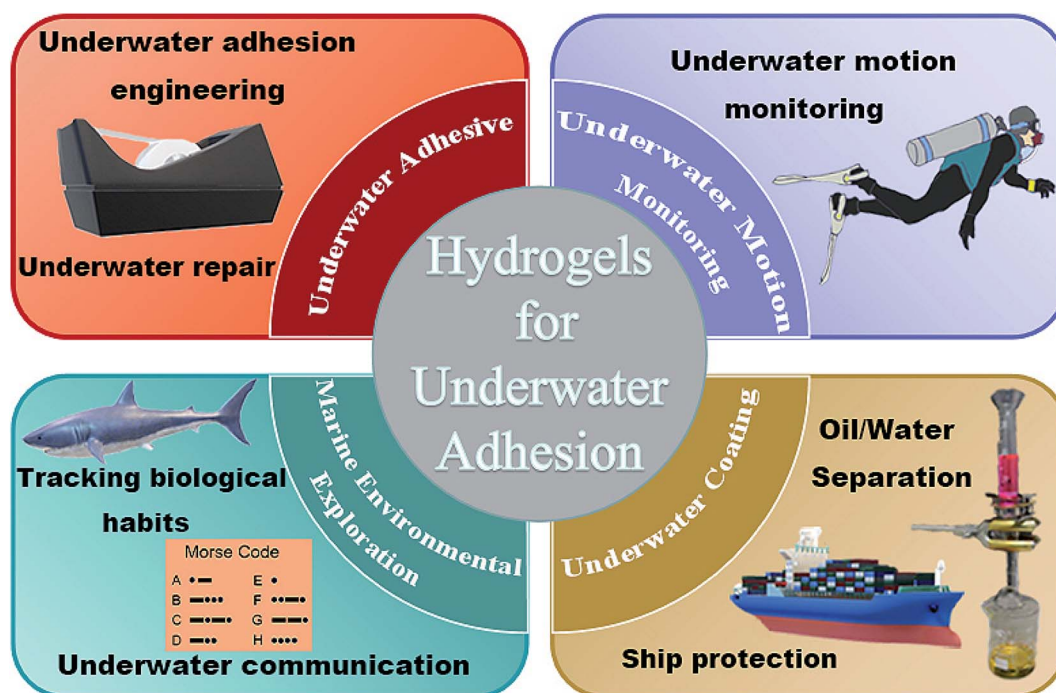


Fig. 7 Various applications of underwater adhesion hydrogels. Figure reproduced with permission from Elsevier and Springer Nature.

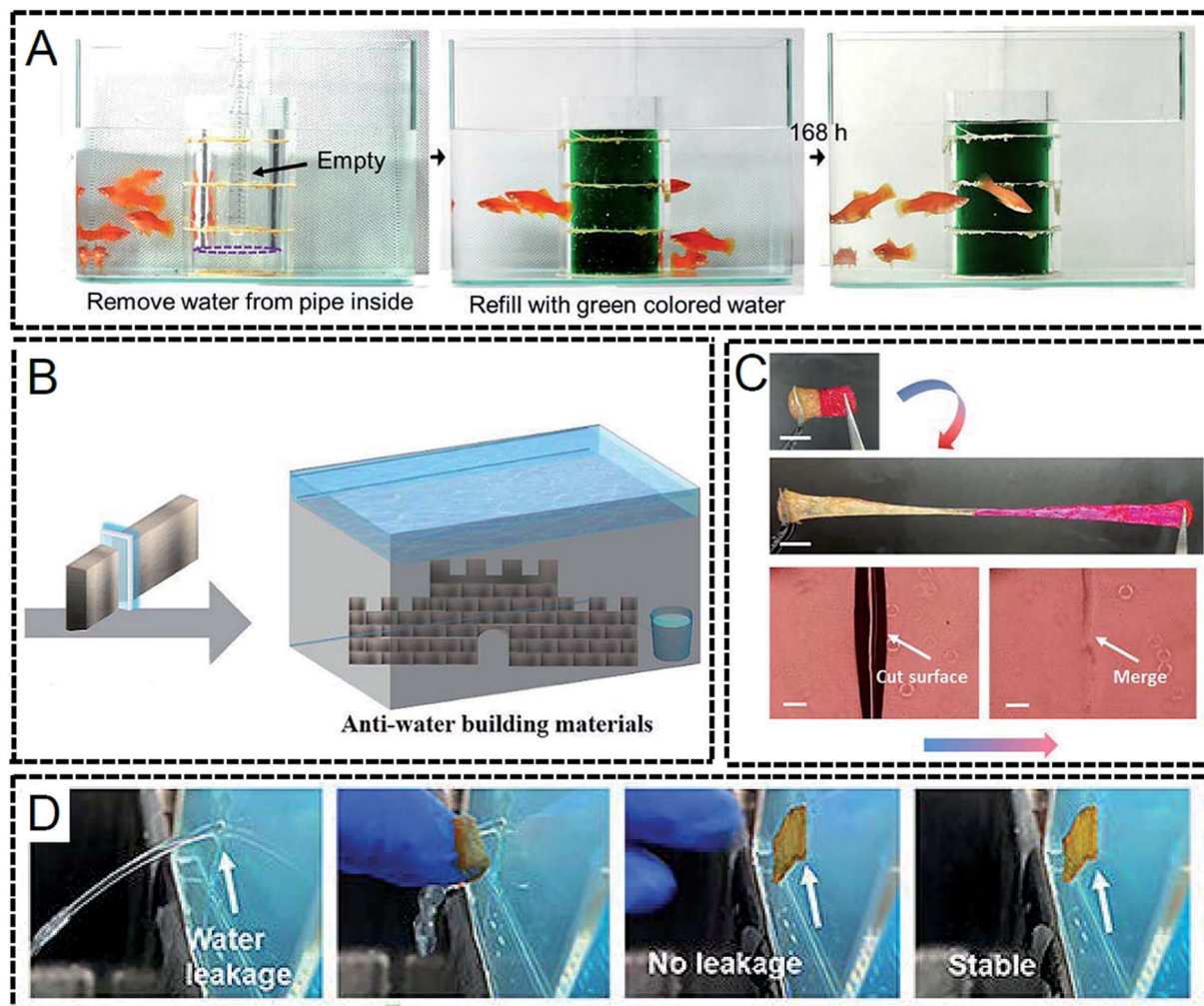


Fig. 8 (A) Adhesives used to bond underwater pipeline interfaces which can ensure a tight bond.<sup>78</sup> Figure reproduced with permission from American Chemical Society. (B) Adhesives are used to bond underwater structures.<sup>141</sup> Figure reproduced with permission from American Chemical Society. (C) Self-healing process of the hydrogel, healing at the incision within a short time after contact.<sup>74</sup> Figure reproduced with permission from American Chemical Society. (D) Underwater adhesive stopping water and repairing a hole.<sup>74</sup> Figure reproduced with permission from American Chemical Society.

practical application. Therefore, how to reduce the impact of adhesive damage is of great significance to ensure the application and engineering stability of underwater equipment. Chen *et al.* developed a highly self-healing polyethylene glycol diacrylate/tannic acid hydrogel using rapid rearrangement of reversible bonds.<sup>74</sup> Therefore, when the hydrogel is damaged, the same hydrogel placed in the original damaged place can be restored to its original state in a short time (Fig. 8C)<sup>74</sup> and maintain the original excellent performance. The reversible non-covalent effect based on the network provides great convenience for repairing defects and avoids unnecessary trouble caused by tedious operation.<sup>146</sup>

Underwater repair is another important field of underwater adhesive application. Rocks, sand and other materials carried by fast-flowing water will have a great impact, and cause holes in the vulnerable parts such as underwater pipelines when they collide. Based on this demand, adhesives that can achieve rapid repair came into being (Fig. 8D).<sup>74</sup> The excellent adhesion

performance of an underwater adhesive ensures that it can effectively prevent leakage and isolate the material inside and outside the hole from each other. Yu *et al.* designed a fluorine-rich ion-rich hydrogel that was applied to a commercial PET film to create waterproof tape, which could stop leaks when attached to a leaky plastic bucket underwater.<sup>100</sup> On the one hand, when applied underwater, the underwater adhesive needs to resist the stresses of the surrounding environment, so the adhesive should have toughness to reduce the risk of brittle fracture and secondary contamination.<sup>43</sup> On the other hand, the remaining underwater adhesives can be recycled and reused after the holes are repaired. Reversible physical adhesion can be achieved through the reconstruction of various physical interactions between the adhesive and interface. The hydrogel designed by Wei *et al.* maintained a stable adhesion after 10 repeated adhesion-peeling experiments, so that the hydrogel could be reused.<sup>76</sup> When applied to underwater repair, it not only reduces the economic loss and environmental pollution



caused by the leak, but also reduces the expenses caused by repair.

The durable and stable underwater adhesive developed through the internal chemical modification of polymers meets the urgent requirements of underwater applications. The new adhesive has great significance for future underwater engineering applications and underwater repair. At the same time, based on the application scenarios of underwater adhesives, how to develop low-cost, environmentally friendly and biosafety adhesives still needs to be explored by researchers.

## 5.2. Underwater motion monitoring

With the improvement of living conditions, more and more people have begun to participate in swimming, diving and other underwater activities, and the hazards caused by discomfort in water are much higher than those on land. In particular, if the overactive muscles twitch, the swimmer will lose the ability to move and call for help, and soon drown. It is of great practical importance to realize real-time monitoring of underwater motion. Gel-based underwater sensing devices have been widely used for underwater motion monitoring (Fig. 9A)<sup>147</sup> because of their remarkable biocompatibility and mechanical characteristics similar to human skin, which adheres well to the skin surface.<sup>148</sup> Hydrogel sensors have potential application value in swimming and diving monitoring.<sup>147</sup> However, in an aquatic environment, the interfacial adhesion may be weakened by the

presence of water at the gel–skin interface, leading to potential end-device delamination and further degradation of data reliability.<sup>93</sup> To meet the demand of underwater sensing, ion-conductive gels with underwater adhesion have been developed in recent years.<sup>149</sup> Interfacial adhesion between human skin and organic hydrogel electronics is necessary for underwater motion monitoring. For instance, Niu *et al.* synthesized an ion-conductive organic hydrogel based on a gelatin–poly(acrylic acid–*N*-hydrosuccinimide ester) (PAA–NHS ester) backbone and a glycerol/water binary solvent system.<sup>150</sup> The covalent bonding between the NHS ester in the gel and the amino group of human skin ensured that the gel achieves strong adhesion to the skin even in water. To further optimize the underwater sensing performance of the hydrogel, the hydrogel was soaked in LiCl solution to obtain LiCl-loaded PAA based hydrogel (L-PAA-OH). Taking advantage of its excellent ductility, conductivity and underwater adhesion, L-PAA-OH was fabricated as an underwater sensor to monitor various underwater motions in real time, showing good linearity, high sensitivity and fast responsiveness.

However, the conductive and sensing properties of conductive gels can easily be lost gradually in an aqueous environment. For example, the polymer chains present in hydrogels readily swell by absorbing water molecules, which can lead to the failure of the gel structure, resulting in unstable sensing performance.<sup>151</sup> In fact, a great deal of effort has been devoted to

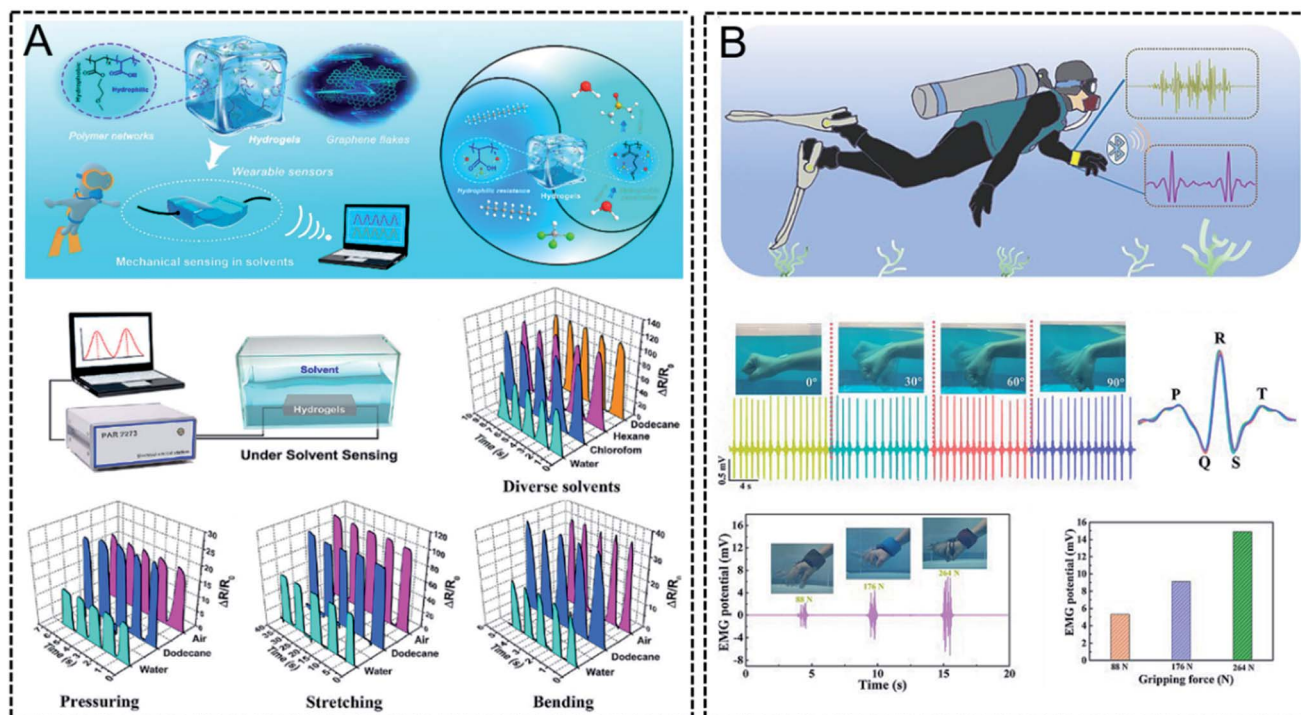


Fig. 9 (A) Schematic diagram of the hydrogel sensor for underwater motion monitoring. Various repeated mechanical deformations of pressure, bending, and stretching in water, dodecane, and air were accurately monitored and reflected by the stable and continuous monitoring signal.<sup>147</sup> Figure reproduced with permission from American Chemical Society. (B) Schematic diagram of BACT gels uses for bioelectric monitoring (ECG and EMG) in the underwater environment. The ECG signals recorded by the BACT gel electrode in the underwater environment during the movement of the wrist. The illustration shows different ECG waveforms produced by BACT gel electrodes at different motion angles.<sup>93</sup> Figure reproduced with permission from Elsevier.

solving the problem of the swelling of hydrogels, and some useful methods have been developed recently, such as solvent-exchange strategies,<sup>147,148,152</sup> high-crosslinking densities<sup>17,153,154</sup> and hydrophobic modification.<sup>37,155</sup> For example, Deng and Cui *et al.* have demonstrated a class of dynamic hydrogels through the Fe<sup>3+</sup>-induced self-hydrophobization process, which endows hydrogels with superior underwater stability and adhesion.<sup>37</sup> These specifically designed anti-swelling hydrogels *via* hydrophobic modification or other strategies can undergo long-term immersion in water. Moreover, the conductive ions in the gel will be lost by diffusion in an aqueous environment, resulting in a gradual loss of conductivity and sensing ability.<sup>35</sup> Therefore, giving ion-conductive gel materials the necessary anti-ion loss capability is of great significance for achieving long-term stable motion monitoring of ion-conductive gel materials underwater and developing wearable underwater sensing technology. Recently, Wei *et al.* developed a fully hydrophobic ionic liquid gel material with long-term stability underwater by exploiting the diffusion barrier function of hydrophobic interfaces for water molecules and conductive ions.<sup>35</sup> In the aqueous environment, the hydrophobic polymer network on the surface of this gel aggregates under hydrophobic action to form a dense hydrophobic interface, which can effectively block the diffusion of water molecules across the interface. Based on the excellent sensing performance and underwater adhesion performance of the fully hydrophobic ionic liquid gel, the gel sensor can not only be attached to the joints of the human body to achieve real-time monitoring of human swimming status (swimming posture, stroke frequency, breathing status, *etc.*).<sup>151,156</sup> The recyclability of gel underwater sensing devices can be further achieved by introducing nanomaterials (metal nanoparticles, graphene,<sup>157–159</sup> *etc.*) into the gel matrix for the synthesis of nanocomposite gels. A nanocomposite hydrogel can form a hydrated layer on the outer surface of the hydrogel. Therefore, it has extremely low protein adsorption capacity, which can effectively reduce bacterial adhesion.<sup>160</sup> Thanks to the non-swelling and anti-fouling properties, the nanocomposite hydrogel can maintain high mechanical strength and sensing performance after 30 days of immersion in water. And it can accurately monitor the submerged fine and huge movements and realize the recyclability of sensing devices.

In addition to real-time underwater motion monitoring by means of transmitting relative resistance changes, underwater real-time electrocardiogram (ECG) monitoring by means of monitoring underwater vital signs such as respiration rate, blood pressure, and cardiac status is another means of underwater motion monitoring (Fig. 9B).<sup>93</sup> Similarly, such a gel device capable of monitoring ECG signals underwater would need to overcome the problems of low adhesion and reduced electrical conductivity of conventional commercial gel electrodes underwater.<sup>93</sup> Recently, Ji *et al.* fabricated a waterproof gel electrode for underwater ECG signal monitoring using an ion-conducting dopamine polymer.<sup>161</sup> The stable underwater conductivity and strong adhesion to the skin enabled the electrode to collect reliable ECG signals under various conditions in water. The wearable device combined with the waterproof electrodes can acquire ECG signals in real time during swimming, which can

be used to reveal heart conditions. The researchers collected ECG signals by adhering the gel electrode device to the human chest underwater and transmitting the signals wirelessly to a mobile-only app. With this setup, ECG signals were recorded before, during and after swimming. The variability of heart rate can be used to warn underwater exercisers of a potential risk of heart attack. In addition, the gel electrodes can be easily peeled off without leaving any residue on the skin and can be reused.

The most important reason why a hydrogel can be an ideal material for underwater motion monitoring is the good coupling with the human skin interface. In the field of underwater motion monitoring, the construction of underwater adhesion hydrogels with high sensitivity and long-term stability will be the focus of future research.

### 5.3. Marine environmental exploration

The ocean is a huge and mysterious treasure, and people never stop exploring and developing it. Diving is one of the most important ways to explore the ocean, but the complex and ever-changing underwater environment harbors various dangers, even threatening the divers' lives. The difficulty of underwater communication makes it difficult for divers to seek help in time when they encounter unexpected situations, further increasing the risk of marine environment exploration. The development of wearable sensing and communication technologies for underwater use, real-time monitoring of the diving process and efficient underwater communication will help to improve the efficiency of marine exploration and ensure the safety of underwater operations. Previously, some underwater sensing hydrogel devices applied to underwater motion monitoring have been developed.<sup>162,163</sup> In practical applications, ionic gel sensors are considered to work stably underwater. Based on their strong underwater adhesion and stable sensing performance, these ionic gel sensing devices allow for unobstructed underwater communication in addition to underwater motion monitoring. The good coupling of the gel to the human skin interface and the stable conduction of resistance changes provides a simple and easy-to-implement idea for underwater communication. By adhering the gel sensor to the human throat area, researchers were able to accurately identify repeatable signals emitted by voice (Fig. 10A).<sup>147</sup> In addition, the sensing device is able to clearly distinguish the signals emitted by different voices.<sup>151,160</sup> In the event of a diver encountering an unexpected situation, the hydrogel sensor can send a timely distress voice. Unlike the detection of speech signals, Wei *et al.* established a novel underwater communication mechanism based on finger joint bending sensing by combining the developed ionic gel skin sensor with the coding principle of Morse code.<sup>35</sup> That is, the large and small bending amplitudes of the finger joints correspond to the long and short message numbers of Morse code, respectively (Fig. 10B).<sup>164</sup> Thus, a wearable underwater transmitter that can be used for underwater communication is constructed. And the underwater sending of messages was initially realized. It is expected to facilitate underwater detection by providing a practical means of underwater communication. In addition to deformation-

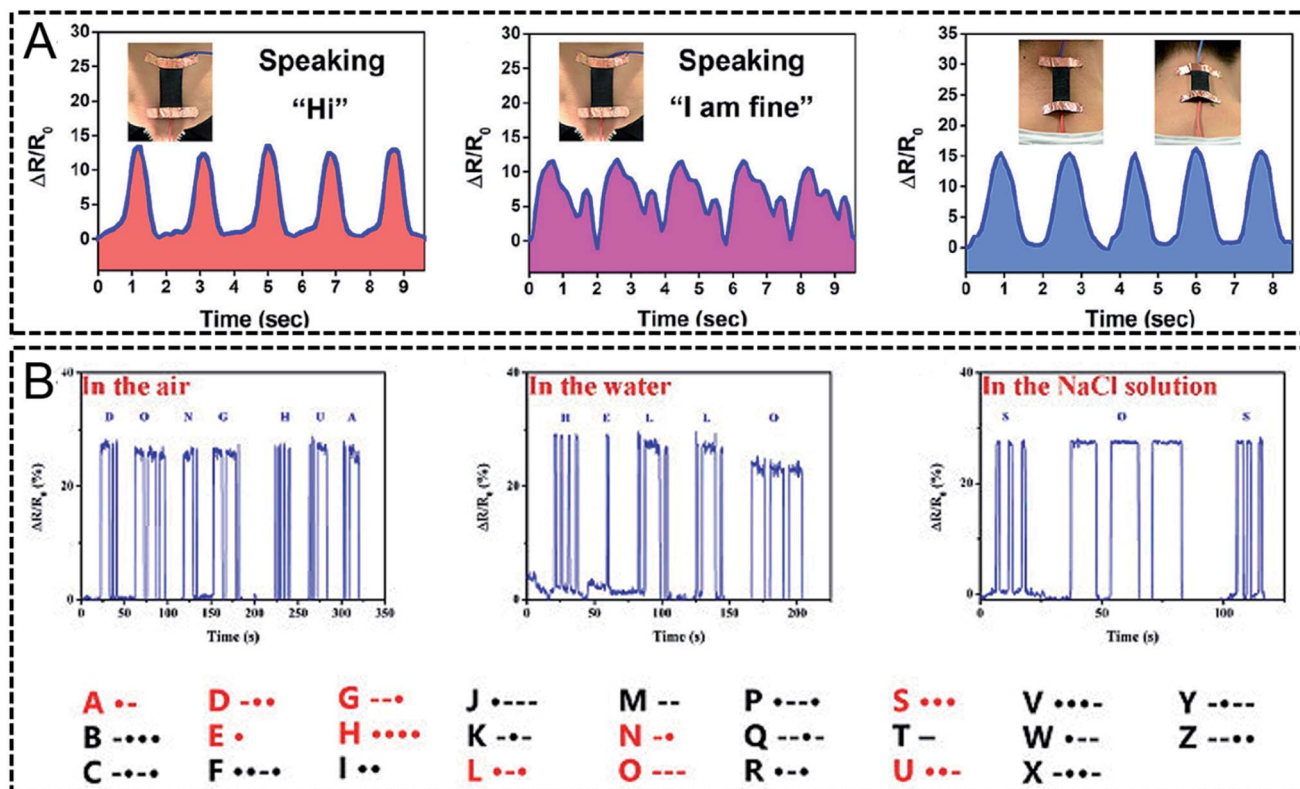


Fig. 10 (A) Schematic diagram of a hydrogel sensor monitoring human voice signals.<sup>147</sup> Figure reproduced with permission from American Chemical Society. (B) Schematic diagram of the hydrogel sensor showing communication through Morse code in the aquatic environment.<sup>164</sup> Figure reproduced with permission from Elsevier.

based signal changes, contactless sensing and information transfer can also be achieved by gel sensors. Yu *et al.* placed gel sensors underwater, and by rhythmically touching the water surface with their fingers and recording different combinations of dashes and dots, information was effectively transferred.<sup>165</sup> The intrinsic mechanism of non-contact sensing is to change the pathway of electron transfer, transferring part of the electron transfer pathway from the sensor to the body, which in turn changes the ground resistance measured by the sensor. Ultimately, non-contact sensing and information transfer between the hand and the sensing device is achieved. It is worth mentioning that this sensing mechanism is based on the excellent sensing performance and strong adhesion of the gel underwater. In addition, the non-contact sensing mode gives the gel sensor excellent fatigue resistance, showing great potential in the field of covert information transmission in the marine environment. The fully hydrophobic ionic gel demonstrates excellent underwater sensing and communication performance in potential marine applications and provides a simple and effective pathway towards next-generation communicators.

At the same time, there has been increasing interest in the exploration and exploitation of the ocean due to its rich resources and biodiversity. The softness, stretchability and biocompatibility of gels have been exploited to develop a variety of gel sensors that can sense stimuli and transmit

information.<sup>166–168</sup> These hydrogel sensors have shown great potential in the field of marine biology research. For example, the developed nanocomposite gel sensor was attached to the oscillating parts of marine animal models such as the tail of sharks by Li *et al.* and was used to monitor their movements in simulated seawater.<sup>160</sup> The gel sensor can clearly distinguish the sensing signals of various motions such as swimming, paddling, and feeding of the marine animal model, enabling accurate monitoring of various continuous and complex motions of underwater animals. Moreover, by identifying the intensity and frequency of the signals, various swimming patterns of marine organisms can be evaluated, including resting, slow swimming, fast swimming, leaping out of the water, and making a right turn and left turn. More importantly, this nanocomposite gel has a strong inhibitory effect on the adhesion of proteins and bacteria, slowing down the formation of biofouling films, and greatly extending the service life of the gel sensor. Through model motion tests and seawater simulations, the gel sensors with excellent underwater adhesion performance, stable sensing performance and tensile resistance have fully demonstrated their great potential in tracking the habits of marine organisms. However, the ecological safety of some gel sensors needs further study, especially in deep-sea environments under high pressure.

Most of the pollution in the ocean comes from human activities, including oil spills, garbage dumping, and domestic



and industrial wastewater discharges.<sup>169–171</sup> The oceans have a considerable impact on the global climate and ecosystem. Although the ocean has a strong self-healing ecosystem, it takes a long time to recover. Therefore, a comprehensive monitoring of the state of the marine environment, especially how human activities affect marine ecosystems, is essential. Recently, a highly resilient, durable, ultra-sensitive ionic gel skin sensor (MIS sensor) based on micro–nanostructures capable of monitoring water wave vibrations was reported.<sup>162</sup> With the well-designed surface structure, the synthesized MIS sensor had excellent flexibility and high sensitivity, which can be attached to human motion joint parts to monitor subtle human motion. More importantly, the sensor had outstanding stimulus response and recognition of multiple stimuli in underwater conditions, which was used to monitor water wave vibrations in real time. The MIS sensor exhibits stable and excellent sensing performance for different frequencies of water waves, and this unique property made the MIS sensor applicable for the monitoring of wave motion at the sea surface. This provides an idea for the development of sensing devices for ocean monitoring. The ocean is rich in biological and mineral resources, and good marine environment monitoring technology is an important technical guarantee for the development of marine resources. In the future, underwater adhesion hydrogel materials are expected to be ideal underwater sensing materials for the development of marine resources. Synthesizing an underwater sensing gel that can conduct stably for a long time and achieve reliable real-time transmission of data will play a very important role in human understanding of the ocean, early warning of catastrophic climate, and environmental protection.

Underwater adhesion hydrogels are used as an ideal underwater sensing material to synthesize underwater sensing devices for different application scenarios. These underwater sensors are equipped with submersibles that can sense underwater at a large and accurate range. Furthermore, the development of sensor technology will be modified and optimized according to the needs of marine development. We summarize the application scenarios of underwater adhesion hydrogel sensors in different fields such as underwater motion monitoring, underwater communication, and marine environmental exploration. Underwater adhesion hydrogel sensors demonstrate excellent sensing and communication performance, providing a simple and effective idea for the development of next-generation wearable underwater sensors and communicators. More notably, the underwater adhesion hydrogel sensors are expected to provide marine environmental monitoring technology and show great potential in the field of marine resource exploitation.

#### 5.4. Underwater coatings

In the past hundred years, the illegal discharge of industrial oily sewage and the frequent occurrence of marine oil spills have caused huge losses to the marine ecological environment and the economic development of the underwater construction industry. The development and application of underwater coatings has received more and more attention and has become

a feasible strategy to deal with the above situations. With its excellent underwater adhesion, oil resistance and anti-biological protein, underwater coatings shine in the fields of underwater building protection and oil/water separation.<sup>172–174</sup> In this section, the advantages of underwater adhesion coatings in the fields of underwater building protection and oil/water separation are summarized in detail, and based on various excellent properties of underwater coatings, a concise overview of the research progress of underwater coatings is given.

As one of the important aspects of underwater building protection, ship protection has high performance requirements for underwater protective coatings. The conventional coating method is to directly coat the prepared underwater coating on the hull, which results in a low adhesion strength of the underwater coating, so it cannot resist the erosion of seawater and the impact of wind and waves. In recent years, researchers have used LBL self-assembly technology to coat the components of the coating layer on the hull (Fig. 11A).<sup>175</sup> This technology not only improves the adhesion of the coating, but also makes the coating have the mortar structure and high surface energy of pearl shells (Fig. 11B),<sup>176</sup> so that the hull can resist the corrosion of oil pollution and the impact of waves in the sea. Some coatings have super strong underwater adhesion and the internal network is dense and compact (Fig. 11C), which prevents the occurrence of ship oil spills from the source, and indirectly protects ships from oil pollution, which can be used in the field of ship leakage prevention.<sup>175</sup> When faced with harsh underwater environments (high content of acids, alkalis and salts), the adhesion properties of underwater coatings can be severely damaged, causing peeling phenomena, exposing ships to harsh environments and accelerating ship corrosion. Therefore, coatings that can survive in harsh environments have been developed,<sup>177–180</sup> and they can still show excellent adhesion and oleophobic properties in harsh environments to protect ships. The vigorous development of the shipping industry in various countries has widened the scope of maritime transportation with the characteristics of spanning latitudes and wide regions. Lower ocean temperatures at high latitudes may cause the coating to freeze, which may affect the underwater adhesion of the coating and accelerate the peeling of the coating. Therefore, coatings with ice resistance were developed.<sup>181</sup> This effectively expanded the application range of underwater adhesive coating in the field of hull protection.

Since metals were discovered and used, metal corrosion has become one of the causes of resource depletion.<sup>182,183</sup> In recent years, the green concept has gradually penetrated into the hearts of people around the world. Offshore wind power generation is one of the important sources of clean energy, due to which the anticorrosion of metal and the metal anticorrosion of power generation equipment have also received attention. Among them, since the underwater zone is immersed in water for a long time and the intermediate transition zone is in close contact with water, the metal corrosion protection of the two is particularly important. Due to the strong adhesion and high pull-out strength of the coating, it is not easy for it to fall off and break when it adheres to the metal surface. The coating can prevent contact between seawater and metal, and has favorable

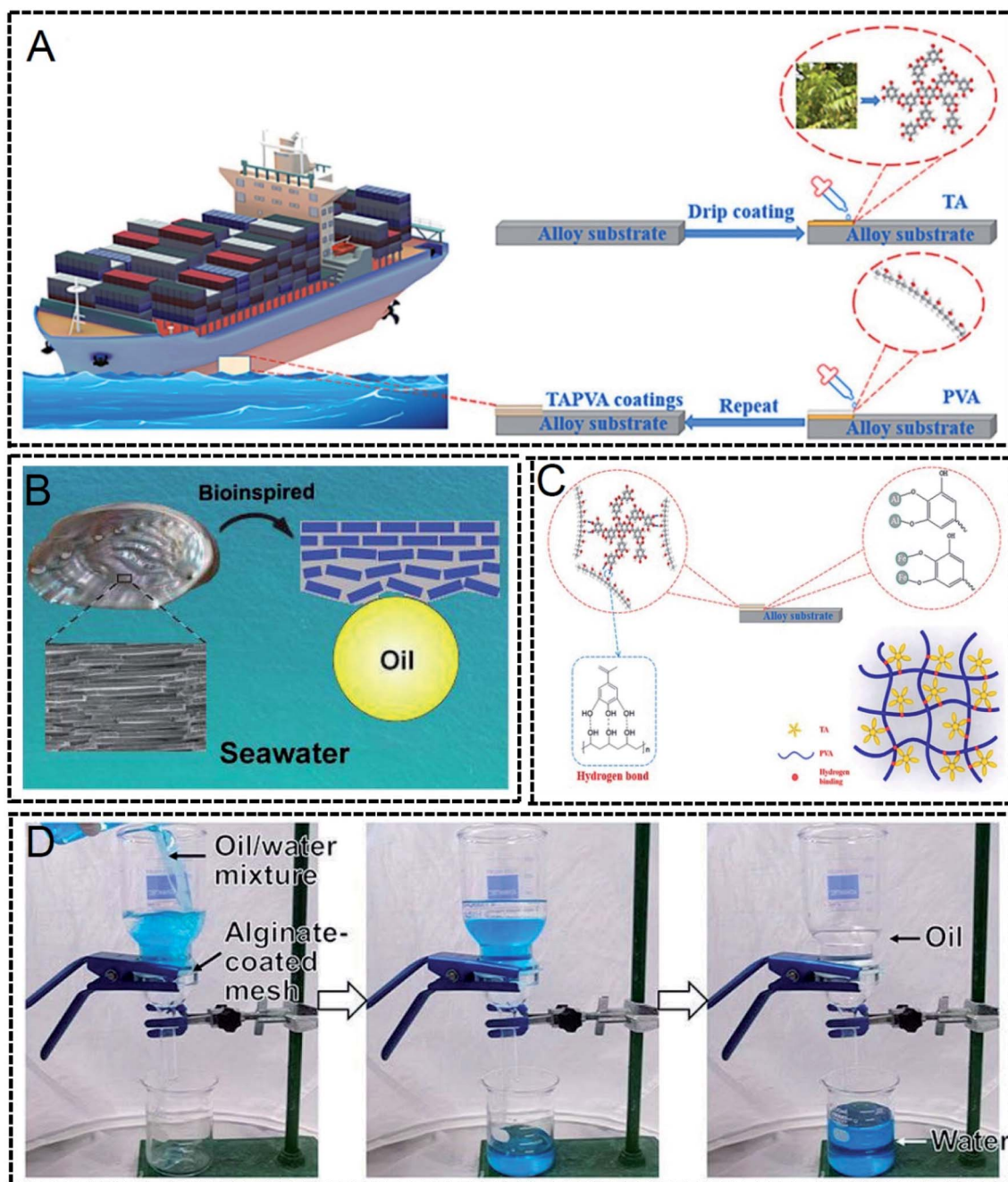


Fig. 11 (A) LBL self-assembly technology used to layer self-assembly coatings onto the hull.<sup>175</sup> Figure reproduced with permission from Elsevier. (B) Imitation pearl mortar structure.<sup>176</sup> Figure reproduced with permission from American Chemical Society. (C) The presence of hydrogen bonds densifying the network of underwater coatings.<sup>175</sup> Figure reproduced with permission from Elsevier. (D) Practical application of underwater coating in oil/water separation.<sup>179</sup> Figure reproduced with permission from American Chemical Society.

anti-corrosion performance.<sup>184</sup> Furthermore, Gu *et al.* found that incorporating multiwall carbon nanotubes into polyester coatings not only imparts properties to the coated metal against corrosion, but also imparts sound-absorbing properties,<sup>185</sup> which may contribute to ocean noise reduction in the future, when sticking it to various objects underwater.

Disposal methods of traditional oil absorbent materials with porous structures (such as foam, sponge, *etc.*) after use, such as

incineration and landfill, will cause environmental pollution. The method by which the coating adhered to the metal mesh is environmentally friendly,<sup>186–188</sup> because the main component of the underwater coating is safe, green and non-toxic. At the same time, due to the excellent water retention of the constituent materials constituting the coating, the retained water will reduce the contact area between the oil and the interface, enabling oil/water separation in the solid/water/oil three-

phase.<sup>189</sup> Once the underwater coating is applied to the metal mesh, only water is allowed to pass through the coating and the metal mesh, and since the density of water is greater than that of oil, the oil/water mixture can be separated only by gravity. This solves the problems of oil clogging and low separation efficiency when simply using interface materials with special wettability for oil/water separation (Fig. 11D).<sup>179,190</sup> The strategy of applying the underwater coating to the metal mesh undoubtedly opens up a new idea for the field of oil/water separation.

In addition, in the process of oil/water separation, because the conditions in some industrial oil-containing wastewater are not mild, and involve high temperature and other harsh environments, adhesion of the underwater coating will be adversely affected and the coating physically damaged. Therefore, it is necessary to prepare underwater coatings with excellent underwater adhesion properties, mechanical properties and oil/water separation ability to adapt to harsh environments. This will reduce the condition requirements for oil/water separation and simplify the oil/water separation.<sup>191,192</sup> However, some harsh environments, such as high content of acid and alkali salts, will cause certain damage to the operator. Therefore, if a stimuli-responsive polymer is introduced into the coating, it can realize remote-control adjustment under its corresponding stimulation conditions (such as magnetic field, electric field, pH, light, heat, *etc.*).<sup>187,189,190,193</sup> The intelligence of the underwater coating for oil/water separation improves the expected oil/water separation effect under certain conditions.

Underwater adhesion is a prerequisite for the application of underwater coatings in the fields of underwater engineering and oil/water separation. Since underwater equipment and underwater engineering are in a complex underwater environment, the stable adhesion of the underwater coating can ensure their normal operation. Due to the precision of oil/water separation work, the coating needs to tightly adhere to the metal mesh to achieve precise separation of oil and water. So far, underwater coatings with various properties, such as sound absorption, noise reduction and intelligent response, have been developed and applied, and innovative new underwater coatings have also relieved people's work. At the same time, the underwater adhesion performance of the underwater coating still needs to be improved, and the underwater coating with long-term stable adhesion performance can be used for a long time under the condition of long-term water scouring.

## 6. Conclusion and outlook

The past decade has witnessed a paradigm shift in the field of synthetic underwater adhesion hydrogels due to the detailed research on the underwater adhesion mechanism of hydrogels. In this review, we provided a comprehensive and systematic summary of the mechanisms of underwater adhesion hydrogels. We briefly outlined methods to enhance underwater adhesion by removing the hydration layer at the molecular and microscopic levels, but efficient drainage of interfacial water at the macroscopic level remains a challenge, especially when bonding large areas. In addition, the effects of forming covalent

bonds and intermolecular forces on interfacial adhesion and hydrogel cohesion were presented in comparison. Although the former is stronger than intermolecular forces, the construction of dynamic covalent bonds and reversible adhesion properties are still important issues to be addressed. We have considered the problem of failure of various intermolecular forces underwater by the disruption of the hydration layer. Based on the proposed underwater adhesion mechanism, the various types of underwater bonded hydrogels we have developed over the last decade are broadly classified into gel-type hydrogels and sol-type hydrogels according to the bonding mode. The design strategies for the different types of hydrogels are summarized in detail based on the different challenges faced in underwater adhesion. For example, for gel-type hydrogels, the key issues of underwater adhesion are hydration layer removal and formation of an effective adhesion interface. Then based on the proposed adhesion mechanism, robust and reproducible underwater adhesion of hydrogel can be achieved by organically combining various methods of hydration layer removal at different levels with the formation of chemical bonding or intermolecular forces. For underwater adhesion guided by bionic microstructures, the preparation process involves complex fabrication and structural design. Typical fabrication methods for artificial underwater adhesion hydrogel surfaces include photolithography, 3D printing and etching, but fabrication methods and special mechanism design are difficult to master. The mechanism of biological surface structure needs to be further explored, and the design of original biological models is needed to improve its underwater adhesion performance. In addition, high-precision measurement instruments need further research to further reveal the biological adhesion structures and potential adhesion mechanisms. In the future, a strategy combining the introduction of microstructure and a molecular level adhesion mechanism will be an effective way to improve the adhesion performance. As for sol-type hydrogels, the curing time can be shortened by introducing external stimuli (light, temperature, pH, and solvent strategies) and reversible adhesion can be achieved by introducing dynamic cross-linking mechanisms. Meanwhile, for two different types of hydrogels, we summarized five different test methods for characterizing the underwater adhesion of hydrogels. Among them, the lap shear test and tack test are more suitable to sol-type hydrogels, while the adhesion test, peel test and tensile test are more suitable to gel-type hydrogels. However, it should be particularly noted that there are significant differences in the magnitude and units of adhesion strength in different studies, and there are human experimental errors during different test operations. Therefore, this review calls for the development of experimental suites with protocols for underwater adhesion measurements. The key to the design of future underwater adhesion hydrogels is the removal of the hydration layer and following multiple design principles, and to achieve this goal, the characterization of the interface between the adhesive and the underwater substrate is crucial. Experimental techniques such as ATRIR, sum-frequency generation spectroscopy, interferometry and ODPN are currently available to characterize the buried adhesive interfaces. However, characterizing the



interface between hydrogels and submerged surfaces has been a huge experimental challenge due to the paucity of research in this area, and there is an urgent need to develop simple microscopic tools to characterize the contact of submerged hydrogels. Furthermore, we believe that a deeper understanding of the underwater mechanism is needed not only from a chemical point of view, but also from mechanical and physical points of view.

Excellent underwater adhesion properties are a prerequisite for hydrogel applications in many fields such as underwater adhesives, underwater motion monitoring, marine environmental exploration and underwater coatings. In order to obtain optimal performance, hydrogels must be given different properties to match the characteristics of the underwater environment in which they are to be applied: electrical conductivity for water-based electronics, stimulus responsiveness for underwater sensors, non-toxicity for marine environmental exploration, and long-term stable adhesion properties for underwater coatings. Low cost, environmentally friendly materials and simple mass production should be considered in the design and manufacture of new underwater adhesives. In the coming years, we expect that underwater adhesion hydrogels will become important tools for underwater soft robots, water-based energy devices, underwater strain sensors, and marine environmental exploration.

## Conflicts of interest

The authors declare no conflict of interest.

## Acknowledgements

The work is financially supported by the National Natural Science Foundation of China (No. 22102067).

## References

- M. Liang, X. Ge, J. Dai, P. Ren, D. Wei, L. Xu, Q. Zhang, C. He, Z. Lu and T. Zhang, *ACS Appl. Bio. Mater.*, 2021, **4**, 5016–5025.
- D. Wang, J. Zhang, Y. Zhong, M. Chu, W. Chang and Z. Yao, *RSC Adv.*, 2018, **8**, 18904–18912.
- Y. Fu, P. Ren, F. Wang, M. Liang, W. Hu, N. Zhou, Z. Lu and T. Zhang, *J. Mater. Chem. B*, 2020, **8**, 2148–2154.
- Y. Xiong, X. Zhang, X. Ma, W. Wang, F. Yan, X. Zhao, X. Chu, W. Xu and C. Sun, *Polym. Chem.*, 2021, **12**, 3721–3739.
- Z. Sun, Z. Li, K. Qu, Z. Zhang, Y. Niu, W. Xu and C. Ren, *J. Mol. Liq.*, 2021, **325**, 115254.
- X. Wang, C. Wei, B. Cao, L. Jiang, Y. Hou and J. Chang, *ACS Appl. Mater. Interfaces*, 2018, **10**, 18338–18350.
- Z. Sun, X. Xie, W. Xu, K. Chen, Y. Liu, X. Chu, Y. Niu, S. Zhang and C. Ren, *ACS Sustainable Chem. Eng.*, 2021, **9**, 12949–12959.
- Z. Li, C. Cui, Z. Zhang, X. Meng, Q. Yan, J. Ouyang, W. Xu, Y. Niu and S. Zhang, *ChemistrySelect*, 2019, **4**, 7838–7843.
- X. Kong, Y. Li, W. Xu, H. Liang, Z. Xue, Y. Niu, M. Pang and C. Ren, *Macromol. Rapid Commun.*, 2021, **42**, 2100416.
- Y. Li, H. Wang, Y. Niu, S. Ma, Z. Xue, A. Song, S. Zhang, W. Xu and C. Ren, *ChemistrySelect*, 2019, **4**, 14036–14042.
- W. Xu, Y. Hong, A. Song and J. Hao, *Colloids Surf., B*, 2020, **185**, 110567.
- Y. Wang, L. Zhang, Y. Guo, Y. Gan, G. Liu, D. Zhang and H. Chen, *Small*, 2021, **17**, 2103423.
- H. Fan, J. Wang, Z. Tao, J. Huang, P. Rao, T. Kurokawa and J. P. Gong, *Nat. Commun.*, 2019, **10**, 5127.
- C. Xie, X. Wang, H. He, Y. Ding and X. Lu, *Adv. Funct. Mater.*, 2020, **30**, 1909954.
- K. Zhang, F. Zhang, Y. Song, J.-B. Fan and S. Wang, *Chin. J. Chem.*, 2017, **35**, 811–820.
- M. A. North, C. A. D. Grosso and J. J. Wilker, *ACS Appl. Mater. Interfaces*, 2017, **9**, 7866–7872.
- H. Fan, J. Wang and J. P. Gong, *Adv. Funct. Mater.*, 2020, **31**, 2009334.
- H. J. Meredith, C. L. Jenkins and J. J. Wilker, *Adv. Funct. Mater.*, 2014, **24**, 3259–3267.
- J. D. White and J. J. Wilker, *Macromolecules*, 2011, **44**, 5085–5088.
- Z. Wang, X. He, T. He, J. Zhao, S. Wang, S. Peng, D. Yang and L. Ye, *ACS Appl. Mater. Interfaces*, 2021, **13**, 36527–36537.
- H. Fan and J. P. Gong, *Adv. Mater.*, 2021, **33**, 2102983.
- A. H. Hofman, I. A. v. Hees, J. Yang and M. Kamperman, *Adv. Mater.*, 2018, **30**, 1704640.
- M. Cui, X. Wang, B. An, C. Zhang, X. Gui, K. Li, Y. Li, P. Ge, J. Zhang, C. Liu and C. Zhong, *Sci. Adv.*, 2019, **5**, eaax3155.
- Q. Zhao, D. W. Lee, B. K. Ahn, S. Seo, Y. Kaufman, J. N. Israelachvili and J. H. Waite, *Nat. Mater.*, 2016, **15**, 407–412.
- J. Xu, X. Li, X. Li, B. Li, L. Wu, W. Li, X. Xie and R. Xue, *Biomacromolecules*, 2017, **18**, 3524–3530.
- Q. Peng, Q. Wu, J. Chen, T. Wang, M. Wu, D. Yang, X. Peng, J. Liu, H. Zhang and H. Zeng, *ACS Appl. Mater. Interfaces*, 2021, **13**, 48239–48251.
- H. Yuk, C. E. Varela, C. S. Nabzdyk, X. Mao, R. F. Padera, E. T. Roche and X. Zhao, *Nature*, 2019, **575**, 169–174.
- X. Peng, X. Xia, X. Xu, X. Yang, B. Yang, P. Zhao, W. Yuan, P. W. Y. Chiu and L. Bian, *Sci. Adv.*, 2021, **7**, eaabe8739.
- X. Fan, Y. Fang, W. Zhou, L. Yan, Y. Xu, H. Zhu and H. Liu, *Mater. Horiz.*, 2021, **8**, 997–1007.
- Y. Wang, V. Kang, W. Federle, E. Arzt and R. Hensel, *Adv. Mater. Interfaces*, 2020, **7**, 2001269.
- Q. Song, Y. Chen, Y. Huang, W. Dan, M. Wang and N. Dan, *Adv. Mater. Technol.*, 2021, **7**, 2100852.
- A. Cholewinski, F. Yang and B. Zhao, *Ind. Eng. Chem. Res.*, 2020, **59**, 15255–15263.
- G. Xia, M. Lin, Y. Jiayu, H. Jinkang, L. Bowen, Y. Mu and X. Wan, *Adv. Mater. Interfaces*, 2021, **8**, 2101544.
- J. Liu, S. Wang, Q. Shen, L. Kong, G. Huang and J. Wu, *ACS Appl. Mater. Interfaces*, 2021, **13**, 1535–1544.
- J. Wei, Y. Zheng and T. Chen, *Mater. Horiz.*, 2021, **8**, 2761–2770.
- C. Cui, C. Fan, Y. Wu, M. Xiao, T. Wu, D. Zhang, X. Chen, B. Liu, Z. Xu, B. Qu and W. Liu, *Adv. Mater.*, 2019, **31**, 1905761.

- 37 L. Han, M. Wang, L. O. Prieto-López, X. Deng and J. Cui, *Adv. Funct. Mater.*, 2020, **30**, 1907064.
- 38 B. Zhang, L. Jia, J. Jiang, S. Wu, T. Xiang and S. Zhou, *ACS Appl. Mater. Interfaces*, 2021, **13**, 36574–36586.
- 39 P. Rao, T. L. Sun, L. Chen, R. Takahashi, G. Shinohara, H. Guo, D. R. King, T. Kurokawa and J. P. Gong, *Adv. Mater.*, 2018, **30**, 1801884.
- 40 F. Pan, S. Ye, R. Wang, W. She, J. Liu, Z. Sun and W. Zhang, *Mater. Horiz.*, 2020, **7**, 2063–2070.
- 41 Y. Zhou, C. Zhang, S. Gao, B. Zhang, J. Sun, J.-j. Kai, B. Wang and Z. Wang, *Chem. Mater.*, 2021, **33**, 8822–8830.
- 42 Z. Wang, L. Guo, H. Xiao, H. Cong and S. Wang, *Mater. Horiz.*, 2020, **7**, 282–288.
- 43 J. Li, A. D. Celiz, J. Yang, Q. Yang, I. Wamala, W. Whyte, B. R. Seo, N. V. Vasilyev, J. J. Vlassak, Z. Suo and D. J. Mooney, *Science*, 2017, **357**, 378–381.
- 44 S. Huang, X. Kong, Y. Xiong, X. Zhang, H. Chen, W. Jiang, Y. Niu, W. Xu and C. Ren, *Eur. Polym. J.*, 2020, **141**, 110094.
- 45 Z. Li, W. Xu, X. Wang, W. Jiang, X. Ma, F. Wang, C. Zhang and C. Ren, *Eur. Polym. J.*, 2021, **146**, 110253.
- 46 Z. Li, X. Meng, W. Xu, S. Zhang, J. Ouyang, Z. Zhang, Y. Liu, Y. Niu, S. Ma, Z. Xue, A. Song, S. Zhang and C. Ren, *Soft Matter*, 2020, **16**, 7323–7331.
- 47 A. Narayanan, A. Dhinojwala and A. Joy, *Chem. Soc. Rev.*, 2021, **50**, 13321–13345.
- 48 H. Yuk, T. Zhang, S. Lin, G. A. Parada and X. Zhao, *Nat. Mater.*, 2016, **15**, 190–196.
- 49 C. Cai, Z. Chen, Y. Chen, H. Li, Z. Yang and H. Liu, *J. Polym. Sci.*, 2021, **59**, 2911–2945.
- 50 Z. Shafiq, J. Cui, L. Pastor-Pérez, V. S. Miguel, R. A. Gropeanu, C. Serrano and A. d. Campo, *Angew. Chem., Int. Ed.*, 2012, **51**, 4332–4335.
- 51 L. Li, W. Smitthipong and H. Zeng, *Polym. Chem.*, 2015, **6**, 353–358.
- 52 L. Li and H. Zeng, *Biotribology*, 2016, **5**, 44–51.
- 53 D. Zhou, S. Li, M. Pei, H. Yang, S. Gu, Y. Tao, D. Ye, Y. Zhou, W. Xu and P. Xiao, *ACS Appl. Mater. Interfaces*, 2020, **12**, 18225–18234.
- 54 C. Heinzmann, C. Weder and L. M. d. Espinosa, *Chem. Soc. Rev.*, 2016, **45**, 342–358.
- 55 Q. Guo, J. Chen, J. Wang, H. Zeng and J. Yu, *Nanoscale*, 2020, **12**, 1307–1324.
- 56 J. H. Waite, *J. Exp. Biol.*, 2017, **220**, 517–530.
- 57 M. J. Harrington, A. Masic, N. Holtén-Andersen, J. H. Waite and P. Fratzl, *Science*, 2010, **328**, 216–220.
- 58 J. Yu, W. Wei, M. S. Menyo, A. Masic, J. H. Waite and J. N. Israelachvili, *Biomacromolecules*, 2013, **14**, 1072–1077.
- 59 S. Bahri, C. M. Jonsson, C. L. Jonsson, D. Azzolini, D. A. Sverjensky and R. M. Hazen, *Environ. Sci. Technol.*, 2011, **45**, 3959–3966.
- 60 S. A. Mian, L.-M. Yang, L. C. Saha, M. A. E. Ahmed and E. Ganz, *Langmuir*, 2014, **30**, 6906–6914.
- 61 B. Yang, C. Lim, D. S. Hwang and H. J. Cha, *Chem. Mater.*, 2016, **28**, 7982–7989.
- 62 J. S. H. Donaldson, S. Das, M. A. Gebbie, M. Rapp, L. C. Jones, Y. Roiter, P. H. Koenig, Y. Gizaw and J. N. Israelachvili, *ACS Nano*, 2013, **7**, 10094–10104.
- 63 J. Saiz-Poseu, J. Mancebo-Aracil, F. Nador, F. Busque and D. Ruiz-Molina, *Angew. Chem., Int. Ed.*, 2019, **58**, 696–714.
- 64 Q. Lu, E. Danner, J. H. Waite, J. N. Israelachvili, H. Zeng and D. S. Hwang, *J. R. Soc. Interface*, 2013, **10**, 20120759.
- 65 Y. Zhou, C. Zhang, S. Gao, W. Li, J.-j. Kai and Z. Wang, *ACS Appl. Mater. Interfaces*, 2021, **13**, 50451–50460.
- 66 J. Yang, R. Bai, B. Chen and Z. Suo, *Adv. Funct. Mater.*, 2019, **30**, 1901693.
- 67 W. Wang, Y. Zhang and W. Liu, *Prog. Polym. Sci.*, 2017, **71**, 1–25.
- 68 M. J. Gilbert, F. Awaja, G. L. Kelly, B. L. Fox, R. Brynolf and P. J. Pigram, *Surf. Interface Anal.*, 2011, **43**, 856–864.
- 69 M. F. Sonnenschein, S. P. Webb, R. C. Cieslinski and B. L. Wendt, *J. Polym. Sci. Pol. Chem.*, 2007, **45**, 989–998.
- 70 Y. Jia, J. Chen, H. Asahara, T.-A. Asoh and H. Uyama, *ACS Appl. Mater. Interfaces*, 2019, **1**, 3452–3458.
- 71 E. David, A. Lazar and A. Armeanu, *J. Mater. Process. Tech.*, 2004, **157–158**, 284–289.
- 72 D. Yang, E. Gustafsson, T. C. Stimpson, A. Esser and R. H. Pelton, *ACS Appl. Mater. Interfaces*, 2017, **9**, 21000–21009.
- 73 C. K. Roy, H. L. Guo, T. L. Sun, A. B. Ihsan, T. Kurokawa, M. Takahata, T. Nonoyama, T. Nakajima and J. P. Gong, *Adv. Mater.*, 2015, **27**, 7344–7348.
- 74 K. Chen, Q. Lin, L. Wang, Z. Zhuang, Y. Zhang, D. Huang and H. Wang, *ACS Appl. Mater. Interfaces*, 2021, **13**, 9748–9761.
- 75 X. Su, W. Xie, P. Wang, Z. Tian, H. Wang, Z. Yuan, X. Liuc and J. Huang, *Mater. Horiz.*, 2021, **8**, 2199–2207.
- 76 X. Wei, D. Chen, X. Zhao, J. Luo, H. Wang and P. Jia, *ACS Appl. Polym. Mater.*, 2021, **3**, 837–846.
- 77 B. Jing, X. Wang, H. Wang, J. Qiu, Y. Shi, H. Gao and Y. Zhu, *J. Phys. Chem. B*, 2017, **121**, 1723–1730.
- 78 D. Lee, H. Hwang, J.-S. Kim, J. Park, D. Youn, D. Kim, J. Hahn, M. Seo and H. Lee, *ACS Appl. Mater. Interfaces*, 2020, **12**, 20933–20941.
- 79 X. Su, Y. Luo, Z. Tian, Z. Yuan, Y. Han, R. Dong, L. Xu, Y. Feng, X. Liu and J. Huang, *Mater. Horiz.*, 2020, **7**, 2651–2661.
- 80 J. Newar, S. Verma and A. Ghatak, *ACS Omega*, 2021, **6**, 15580–15589.
- 81 Q. Peng, J. Chen, T. Wang, L. Gong, X. Peng, M. Wu, Y. Ma, F. Wu, D. Yang, H. Zhang and H. Zeng, *J. Mater. Chem. A*, 2021, **9**, 12988–13000.
- 82 R. Zhang, H. Peng, T. Zhou, Y. Yao, X. Zhu, B. Bi, X. Zhang, B. Liu, L. Niu and W. Wang, *ACS Appl. Polym. Mater.*, 2019, **1**, 2883–2889.
- 83 H. Wang, X. Su, Z. Chai, Z. Tian, W. Xie, Y. Wang, Z. Wan, M. Deng, Z. Yuan and J. Huang, *Chem. Eng. J.*, 2022, **428**, 131049.
- 84 Y. Chen, X. Guo, A. Mensah, Q. Wang and Q. Wei, *ACS Appl. Mater. Interfaces*, 2021, **13**, 59761–59771.
- 85 L. Meng, C. Shao, C. Cui, F. Xu, J. Lei and J. Yang, *ACS Appl. Mater. Interfaces*, 2020, **12**, 1628–1639.
- 86 X. Liu, Q. Zhang, L. Duan and G. Gao, *ACS Appl. Mater. Interfaces*, 2019, **11**, 6644–6651.



- 87 M. Shin, Y. Park, S. Jin, Y. M. Jung and H. J. Cha, *Chem. Mater.*, 2021, **33**, 3196–3206.
- 88 M. A. Gebbie, W. Wei, A. M. Schrader, T. R. Cristiani, H. A. Dobbs, M. Idso, B. F. Chmelka, J. H. Waite and J. N. Israelachvili, *Nat. Chem.*, 2017, **9**, 473–479.
- 89 N. Holten-Andersen, M. J. Harrington, H. Birkedal, B. P. Lee, P. B. Messersmith, K. Y. C. Lee and H. Waite, *Proc. Natl. Acad. Sci. U. S. A.*, 2011, **108**, 2651–2655.
- 90 M. Liang, C. He, J. Dai, P. Ren, Y. Fu, F. Wang, X. Ge, T. Zhang and Z. Lu, *J. Mater. Chem. B*, 2020, **8**, 8232–8241.
- 91 Y. Bu, L. Zhang, J. Liu, L. Zhang, T. Li, H. Shen, X. Wang, F. Yang, P. Tang and D. Wu, *ACS Appl. Mater. Interfaces*, 2016, **8**, 12674–12683.
- 92 S. Kaur, A. Narayanan, S. Dalvi, Q. Liu, A. Joy and A. Dhinojwala, *ACS Cent. Sci.*, 2018, **4**, 1420–1429.
- 93 C. Sun, J. Luo, T. Jia, C. Hou, Y. Li, Q. Zhang and H. Wang, *Chem. Eng. J.*, 2022, **431**, 134012.
- 94 M. Pan, K.-C. T. Nguyen, W. Yang, X. Liu, X.-Z. Chen, P. W. Major, L. H. Le and H. Zeng, *Chem. Eng. J.*, 2022, **434**, 134418.
- 95 Z. Wang, J. Zhao, W. Tang, T. He, S. Wang, X. He, Y. Chen, D. Yang and S. Peng, *ACS Appl. Mater. Interfaces*, 2021, **13**, 3435–3444.
- 96 Y. Xu, Y. Ji and J. Ma, *Langmuir*, 2021, **37**, 311–321.
- 97 H. Qiao, P. Qi, X. Zhang, L. Wang, Y. Tan, Z. Luan, Y. Xia, Y. Li and K. Sui, *ACS Appl. Mater. Interfaces*, 2019, **11**, 7755–7763.
- 98 P. Karnal, A. Jha, H. Wen, S. Gryska, C. Barrios and J. Frechette, *Langmuir*, 2019, **35**, 5151–5161.
- 99 M. Dompé, F. J. Cedano-Serrano, M. Vahdati, L. Westerveld, D. Hourdet, C. Creton, J. Gucht, T. Kodger and M. Kamperman, *Adv. Mater. Interfaces*, 2019, **7**, 1901785.
- 100 Z. Yu and P. Wu, *Mater. Horiz.*, 2021, **8**, 2057–2064.
- 101 Z. Zhang, L. Guo and J. Hao, *ACS Appl. Polym. Mater.*, 2021, **3**, 3060–3070.
- 102 J. Yu, B. Cheng and H. Ejima, *J. Mater. Chem. B*, 2020, **8**, 6798–6801.
- 103 V. Nele, J. P. Wojciechowski, J. P. K. Armstrong and M. M. Stevens, *Adv. Funct. Mater.*, 2020, **30**, 2002759.
- 104 X. Fan, W. Zhou, Y. Chen, L. Yan, Y. Fang and H. Liu, *ACS Appl. Mater. Interfaces*, 2020, **12**, 32031–32040.
- 105 R. Wang, J. Li, W. Chen, T. Xu, S. Yun, Z. Xu, Z. Xu, T. Sato, B. Chi and H. Xu, *Adv. Funct. Mater.*, 2017, **27**, 1604894.
- 106 X. N. Zhang, Y. J. Wang, S. Sun, L. Hou, P. Wu, Z. L. Wu and Q. Zheng, *Macromolecules*, 2018, **51**, 8136–8146.
- 107 G. Huang, Z. Tang, S. Peng, P. Zhang, T. Sun, W. Wei, L. Zeng, H. Guo, H. Guo and G. Meng, *Macromolecules*, 2021, **55**, 156–165.
- 108 S. Baik, G. W. Hwang, S. Jang, S. Jeong, K. H. Kim, T.-H. Yang and C. Pang, *ACS Appl. Mater. Interfaces*, 2021, **13**, 6930–6940.
- 109 S. Baik, D. W. Kim, Y. Park, T.-J. Lee, S. Ho Bhang and C. Pang, *Nature*, 2017, **546**, 396–400.
- 110 B. Zhao, N. Pesika, K. Rosenberg, Y. Tian, H. Zeng, P. McGuiggan, K. Autumn and J. Israelachvili, *Langmuir*, 2008, **24**, 1517–1524.
- 111 W. Federle, W. J. P. Barnes, W. Baumgartner, P. Drechsler and J. M. Smith, *J. R. Soc. Interface*, 2006, **3**, 689–697.
- 112 S. H. Lee, H. W. Song, B. S. Kang and M. K. Kwak, *ACS Appl. Mater. Interfaces*, 2019, **11**, 47571–47576.
- 113 K. Tsujioka, Y. Matsuo, M. Shimomura and Y. Hirai, *Langmuir*, 2022, **38**, 1215–1222.
- 114 Y. Ma, S. Ma, Y. Wu, X. Pei, S. N. Gorb, Z. Wang, W. Liu and F. Zhou, *Adv. Mater.*, 2018, **30**, 1801595.
- 115 Z. Geng, Z. Li, Z. Cui, J. Wang, X. Yang and C. Liu, *Nano Lett.*, 2020, **20**, 7716–7721.
- 116 H. Chen, L. Zhang, D. Zhang, P. Zhang and Z. Han, *ACS Appl. Mater. Interfaces*, 2015, **7**, 13987–13995.
- 117 H. E. Jeong and K. Y. Suh, *Nano Today*, 2009, **4**, 335–346.
- 118 Y.-C. Chuanga, H.-K. Changa, G.-L. Liu and P.-Y. Chen, *J. Mech. Behav. Biomed. Mater.*, 2017, **73**, 76–85.
- 119 D. Das and T. C. Nag, *Zoology*, 2006, **109**, 300–309.
- 120 W. E. Cloete and W. W. Focke, *Int. J. Adhes. Adhes.*, 2010, **30**, 208–213.
- 121 X. Li, W. Li, Z. Liu, X. Wang, H. Guo, R. Wang, X. Guo, C. Li and X. Jia, *J. Appl. Polym. Sci.*, 2018, **135**, 46579.
- 122 J. Zhou, Y. Wan, N. Liu, H. Yin, B. Li, D. Sun and Q. Ran, *J. Appl. Polym. Sci.*, 2018, **135**, 45688.
- 123 S. Panchireddy, B. Grignard, J.-M. Thomassin, C. Jerome and C. Detrembleur, *ACS Sustainable Chem. Eng.*, 2018, **6**, 14936–14944.
- 124 H. J. Kim, B. H. Hwang, S. Lim, B.-H. Choi, S. H. Kang and H. J. Cha, *Biomaterials*, 2015, **72**, 104–111.
- 125 Y. Akdogan, W. Wei, K.-Y. Huang, Y. Kageyama, E. W. Danner, D. R. Miller, N. R. M. Rodriguez, J. H. Waite and S. Han, *Angew. Chem., Int. Ed.*, 2014, **53**, 11253–11256.
- 126 B. K. Ahn, S. Das, R. Linstadt, Y. Kaufman, N. R. Martinez-Rodriguez, R. Mirshafian, E. Kesselman, Y. Talmon, B. H. Lipshutz, J. N. Israelachvili and J. H. Waite, *Nat. Commun.*, 2015, **6**, 8663.
- 127 S. Seo, D. W. Lee, J. S. Ahn, K. Cunha, E. Filippidi, S. W. Ju, E. Shin, B. S. Kim, Z. A. Levine, R. D. Lins, J. N. Israelachvili, J. H. Waite, M. T. Valentine, J. E. Shea and B. K. Ahn, *Adv. Mater.*, 2017, **29**, 1703026.
- 128 C. Wei, X. Zhu, H. Peng, J. Chen, F. Zhang and Q. Zhao, *ACS Sustainable Chem. Eng.*, 2019, **7**, 4508–4514.
- 129 W. Zhang, R. Wang, Z. Sun, X. Zhu, Q. Zhao, T. Zhang, A. Cholewinski, F. K. Yang, B. Zhao, R. Pinnaratip, P. K. Forooshanie and B. P. Lee, *Chem. Soc. Rev.*, 2020, **49**, 433–464.
- 130 D. Aoki and H. Ajiro, *Macromol. Rapid Commun.*, 2021, **42**, 2100128.
- 131 Y. Yan, J. Huang, X. Qiu, D. Zhuang, H. Liu, C. Huang, X. Wu and X. Cui, *Chem. Eng. J.*, 2022, **431**, 133460.
- 132 S. Rose, A. PrevotEAU, P. Elzie' re, D. Hourdet, A. Marcellan and L. Leibler, *Nature*, 2014, **505**, 382–385.
- 133 Y. Zhao, Y. Wu, L. Wang, M. Zhang, X. Chen, M. Liu, J. Fan, J. Liu, F. Zhou and Z. Wang, *Nat. Commun.*, 2017, **8**, 2218.
- 134 K. Tian, J. Bae, Z. Suo and J. J. Vlassak, *ACS Appl. Mater. Interfaces*, 2018, **10**, 43252–43261.
- 135 J. Tang, J. Li, J. J. Vlassak and Z. Suo, *Soft Matter*, 2016, **12**, 1093–1099.

- 136 H. Yi, S. H. Lee, M. Seong, M. K. Kwak and H. E. Jeong, *J. Mater. Chem. B*, 2018, **6**, 8064–8070.
- 137 L. Xie, L. Gong, J. Zhang, L. Han, L. Xiang, J. Chen, J. Liu, B. Yan and H. Zeng, *J. Mater. Chem. A*, 2019, **7**, 21944–21952.
- 138 R. E. Messersmith, M. E. Bartlett, D. J. Rose, D. A. Smith, M. W. Patchan, J. J. Benkoski, M. M. Trexler and C. M. Hoffman, *ACS Appl. Polym. Mater.*, 2021, **3**, 996–1002.
- 139 A. Cholewinski, F. Yang and B. Zhao, *Mater. Horiz.*, 2019, **6**, 285–293.
- 140 R. J. Stewart, T. C. Ransom and V. Hlady, *J. Polym. Sci. Pol. Phys.*, 2011, **49**, 757–771.
- 141 S. Gu, J. Liu, J. Zheng, H. Wang and J. Wu, *ACS Appl. Mater. Interfaces*, 2021, **13**, 43404–43413.
- 142 X. Yin, Y. Zhang, P. Lin, Y. Liu, Z. Wang, B. Yu, F. Zhou and Q. Xue, *J. Mater. Chem. A*, 2017, **5**, 1221–1232.
- 143 L. Han, L. Yan, K. Wang, L. Fang, H. Zhang, Y. Tang, Y. Ding, L.-T. Weng, J. Xu, J. Weng, Y. Liu, F. Ren and X. Lu, *NPG Asia Mater.*, 2017, **9**, e372.
- 144 W. Wei, J. Yu, C. Broomell, J. N. Israelachvili and J. H. Waite, *J. Am. Chem. Soc.*, 2013, **135**, 377–383.
- 145 B. J. Kim, D. X. Oh, S. Kim, J. H. Seo, D. S. Hwang, A. Masic, D. K. Han and H. J. Cha, *Biomacromolecules*, 2014, **15**, 1579–1585.
- 146 C. Shao, M. Wang, H. Chang, F. Xu and J. Yang, *ACS Sustainable Chem. Eng.*, 2017, **5**, 6167–6174.
- 147 X. Liu, Q. Zhang and G. Gao, *ACS Nano*, 2020, **14**, 13709–13717.
- 148 L. Xu, S. Gao, Q. Guo, C. Wang, Y. Qiao and D. Qiu, *Adv. Mater.*, 2020, **32**, 2004579.
- 149 L. Xu, Z. Huang, Z. h. Deng, Z. Du, T. L. Sun, Z.-H. Guo and K. Yue, *Adv. Mater.*, 2021, **33**, 2105306.
- 150 Y. Niu, H. Liu, R. He, M. Luo, M. Shu and F. Xu, *Small*, 2021, **17**, 2101151.
- 151 J. Ren, Y. Liu, Z. Wang, S. Chen, Y. Ma, H. Wei and S. Lü, *Adv. Funct. Mater.*, 2021, 2107404, DOI: [10.1002/adfm.202107404](https://doi.org/10.1002/adfm.202107404).
- 152 X. Liu, Q. Zhang, F. Jia and G. Gao, *Sci. China Mater.*, 2021, **64**, 3069–3078.
- 153 H. Fan, J. Wang and Z. Jin, *Macromolecules*, 2018, **51**, 1696–1705.
- 154 Z. Xu, C. Fan, Q. Zhang, Y. Liu, C. Cui, B. Liu, T. Wu, X. Zhang and W. Liu, *Adv. Funct. Mater.*, 2021, **31**, 2100462.
- 155 Y. Wang, X. Yao, S. Wu, Q. Li, J. Lv, J. Wang and L. Jiang, *Adv. Mater.*, 2017, **29**, 1700865.
- 156 X. Sun, S. He, Z. Qin, J. Li and F. Yao, *Compos. Commun.*, 2021, **26**, 100784.
- 157 M. Karimi, P. S. Zangabad, S. Baghaee-Ravari, M. Ghazadeh, H. Mirshekari and M. R. Hamblin, *J. Am. Chem. Soc.*, 2017, **139**, 4584–4610.
- 158 H. Liao, X. Guo, P. Wan and G. Yu, *Adv. Funct. Mater.*, 2019, **29**, 1904507.
- 159 W. Zhao, X. Qu, Q. Xu, Y. Lu, W. Yuan, W. Wang, Q. Wang, W. Huang and X. Dong, *Adv. Electron. Mater.*, 2020, **6**, 2000267.
- 160 S. He, X. Sun, Z. Qin, X. Dong, H. Zhang, M. Shi, F. Yao, H. Zhang and J. Li, *Adv. Mater. Technol.*, 2021, 2101343, DOI: [10.1002/admt.202101343](https://doi.org/10.1002/admt.202101343).
- 161 S. Ji, C. Wan, T. Wang, Q. Li, G. Chen, J. Wang, Z. Liu, H. Yang, X. Liu and X. Chen, *Adv. Mater.*, 2020, **32**, 2001496.
- 162 L. Ma, J. Wang, J. He, Y. Yao, X. Zhu, L. Peng, J. Yang, X. Liu and M. Qu, *J. Mater. Chem. A*, 2021, **9**, 26949–26962.
- 163 Y. Cheng, C. Huang, D. Yang, K. Ren and J. Wei, *J. Mater. Chem. B*, 2018, **6**, 8170–8179.
- 164 J. Tie, Z. Mao, L. Zhang, Y. Zhong, X. Sui and H. Xu, *Compos. B. Eng.*, 2022, **232**, 109612.
- 165 Z. Yu and P. Wu, *Adv. Mater.*, 2021, **33**, 2008479.
- 166 D. Chen and Q. Pei, *Chem. Rev.*, 2017, **117**, 11239–11268.
- 167 M. L. Hammock, A. Chortos, B. C.-K. Tee, J. B.-H. Tok and Z. Bao, *Adv. Mater.*, 2013, **25**, 5997–6038.
- 168 X.-F. Zhao, C.-Z. Hang, H.-L. Lu, K. Xu, H. Zhang, F. Yang, R.-G. Ma, J.-C. Wang and D. W. Zhang, *Nano Energy*, 2020, **68**, 104346.
- 169 K. Lin, W. Sun, L. Feng, H. Wang, T. Feng, J. Zhang, M. Cao, S. Zhao, Y. Yuan and N. Wang, *Chem. Eng. J.*, 2022, **430**, 133121.
- 170 K. Richardson, D. Haynes, A. Talouli and M. Donoghue, *Ambio*, 2017, **46**, 190–200.
- 171 K. Sun, W. Cui and C. Chen, *Sensors-Basel*, 2021, **21**, 7849.
- 172 T. Guo, L. Heng, M. Wang, J. Wang and L. Jiang, *Adv. Mater.*, 2016, **28**, 8505–8510.
- 173 X. C. Xia, X. K. Cao, G. Y. Cai, D. Jiang, F. Zhang and Z. H. Dong, *Colloid. Surf., A*, 2021, **628**, 127323.
- 174 D. Zhang, Z. Liu, G. Wu, Z. Yang, Y. Cui, H. Li and Y. Zhang, *ACS Appl. Bio. Mater.*, 2021, **4**, 6351–6360.
- 175 N. Yang, R. Yuan, D. You, Q. Zhang, J. Wang, H. Xuan and L. Ge, *Colloid. Surf., A*, 2022, **634**, 127948.
- 176 L.-P. Xu, J. Peng, Y. Liu, Y. Wen, X. Zhang, L. Jiang and S. Wang, *ACS Nano*, 2013, **7**, 5077–5083.
- 177 K. Chen, S. Zhou and L. Wu, *ACS Nano*, 2016, **10**, 1386–1394.
- 178 Z. Liao, G. Wu, D. Lee and S. Yang, *ACS Appl. Mater. Interfaces*, 2019, **11**, 13642–13651.
- 179 T. Matsubayashi, M. Tenjimbayashi, M. Komine, K. Manabe and S. Shiratori, *Ind. Eng. Chem. Res.*, 2017, **56**, 7080–7085.
- 180 C. Wang, F. Zhang, C. Yu and S. Wang, *ACS Appl. Mater. Interfaces*, 2020, **12**, 42430–42436.
- 181 M.-Q. Ma, C. Zhang, T.-T. Chen, J. Yang, J.-J. Wang, J. Ji and Z.-K. Xu, *Langmuir*, 2019, **35**, 1895–1901.
- 182 Z. Zhang, Z. Li, Y. Hu, A. Song, Z. Xue, Y. Li, Z. Sun, X. Kong, W. Xu and S. Zhang, *Appl. Phys. A*, 2019, **125**, 588.
- 183 W. Xu, Y. Hu, W. Bao, X. Xie, Y. Liu, A. Song and J. Hao, *Appl. Surf. Sci.*, 2017, **399**, 491–498.
- 184 A. W. Momber, P. Plagemann and V. Stenzel, *Int. J. Adhes. Adhes.*, 2016, **65**, 96–101.
- 185 B.-E. Gu, C.-Y. Huang, T.-H. Shen and Y.-L. Lee, *Prog. Org. Coat.*, 2018, **121**, 226–235.
- 186 Y. Liu, L. Wang, H. Lu and Z. Huang, *ACS Appl. Polym. Mater.*, 2020, **2**, 4770–4778.
- 187 Y. Cao, N. Liu, C. Fu, K. Li, L. Tao, L. Feng and Y. Wei, *ACS Appl. Mater. Interfaces*, 2014, **6**, 2026–2030.

## Review

- 188 J.-J. Li, Y.-N. Zhou and Z.-H. Luo, *Prog. Polym. Sci.*, 2018, **87**, 1–33.
- 189 Z. Xue, S. Wang, L. Lin, L. Chen, M. Liu, L. Feng and L. Jiang, *Adv. Mater.*, 2011, **23**, 4270–4273.
- 190 Y. Lv, X. Xi, L. Dai, S. Tong and Z. Chen, *Adv. Mater. Interfaces*, 2021, **8**, 2002030.
- 191 J. Wang, S. Liu and S. Guo, *Appl. Surf. Sci.*, 2020, **503**, 144180.
- 192 Y. Liu, M. Xia, L. Wu, S. Pan, Y. Zhang, B. He and P. He, *Ind. Eng. Chem. Res.*, 2019, **58**, 21649–21658.
- 193 T. Li, J. Shen, Z. Zhang, S. Wang and D. Wei, *RSC Adv.*, 2016, **6**, 40656–40663.